Biointerface Research in Applied Chemistry
Open-Access Journal (ISSN: 2069-5837)

Article
Volume 13, Issue 6, 2023, 573
https://doi.org/10.33263/BRIAC136.573

Novel Edible Bionanocomposites Films Based on Lemon Grass Nanoemulsion and ZnO-NPs for Extending the Shelf Life of Chilled Chicken Meat

Amal W. Ayoub [1], Sherief M. Sayed [2], Mahmoud A. Ammar [1], Yehia A. Hefnawy [2], Ahmed M. Youssef [3,*]

[1] Certified Food Lab, Animal Health Research Institute (AHRI), Agricultural Research Center (ARC), Egypt, Assiut lab.; amlwahid79@yahoo.com (A.W.A.); mahmoud2014eg@yahoo.com (M.A.A.);
[2] Meat Hygiene and Technology, Food Hygiene Department, Faculty of Veterinary Medicine – Assiut University, Assiut 71526, Egypt; shsayed74@aun.edu.eg (S.M.S.); hefnawy51@aun.edu.eg (Y.A.H.);
[3] Packaging Materials Department, National Research Centre, 33 El Bohouth St. (former El Tahrir st.), Dokki, Giza, Egypt, P.O. 12622; amyoussef27@yahoo.com (A.M.Y.);
* Correspondence: amyoussef27@yahoo.com (A.M.Y.);

Scopus Author ID 55619673300
Received: 8.11.2022; Accepted: 7.03.2023; Published: 26.03.2023

Abstract: In the current work, novel bionanocomposite based on chitosan (CS), polyvinyl alcohol (PVA), and gelatin (GE), incorporating lemon grass nanoemulsion (Lg-NE) and zinc oxide nanoparticles (ZnO-NPs). The prepared ZnO-NPs and Lg-NE morphology were evaluated using a transmission electron microscope (TEM), and the drop particle size was assessed using dynamic light scattering (DLS). The fabricated CS/PVA/GE/ZnO/Lg bionanocomposites were assessed using X-ray diffraction pattern (XRD), scanning electron microscope (SEM), Fourier-transform infrared spectroscopy (FTIR) and were evaluated for their antimicrobial effect. The permeability, thermal and mechanical properties of the films were evaluated. The oxygen transmission rate (OTR), water vapor transmission rate (WVTR), thermal, mechanical, and antimicrobial properties of fabricated CS/PVA/GE/ZnO/Lg bionanocomposite were enhanced through the addition of Lg-NE (13.8, 20, and 25% (v/w)) and ZnO-NPs (2% w/w). The influences of Lg-NE and ZnO-NPs in a mixture combined into a CS/PVA/GE blend as an edible film on the shelf life of chilled chicken meat and their quality throughout refrigerated storage (4±2 ºC) were evaluated for 7 days of storage. The obtained results designated that ZnO-NPs combined with Lg-NE have a synergistic effect on the improvement of the CS/PVA/GE/ZnO/Lg bionanocomposite preservation properties for refrigerated chilled chicken meat, compared with those without ZnO-NPs and Lg-NE, as they extend the shelf life of samples, enhances their sensory characteristics, pH, Thiobarbituric acid reactive substances (TBARS) value, and also have a prominent influence on the microbiological condition of samples. Furthermore, the prepared nanocomposites have a marked effect on the population of pathogenic food microorganisms, *Listeria monocytogenes* and *Salmonella Typhimurium*, through the chilled chicken meat storage period.

Keywords: lemon grass nanoemulsion; ZnO-NPs; bionanocomposites film; chilled chicken meat; Packaging; SEM; mechanical; thermal properties; microbiological analysis.

1. Introduction

Chicken meat occupies the top position in the human consumption of meat. This is because it is affordable, takes a short production cycle, is easy to be prepared, has high nutritional value, and contains low-fat content [1]. However, chicken meat is liable to bacterial spoilage and lipid oxidation due to its nutritional components and high pH levels [2]. Recently,

great attention has been paid to replacing traditional plastic-based food packaging with bio-based and biodegradable active films [3]. This technology allows placing a physical barrier on the food surface, reducing moisture and solutes migration as well as gas exchange, preventing oxidative reactions and food deterioration during storage. Furthermore, the use of active edible films comprising antimicrobial agents used for preserving foodstuffs represents a novel method for improving the shelf life of foodstuffs [4].

Hydrocolloids (proteins and polysaccharides) such as chitosan and gelatin or a combination of them are considered the highly recommended biodegradable materials used in packaging meat, fish, and poultry products [5,6]. This is returned to their sustainability, abundance, compostability, eco-friendly, compatibility with foodstuffs, and food applications. In addition to their bio-functionality, film-forming capacity, and antimicrobial properties[7,8] However, the biopolymers show poor barrier, mechanical, and processing properties with high production costs compared with petroleum-based plastic materials [9]. These limitations can be modified by adding plasticizers, surfactants, cross-linkers, antimicrobial agents, functional additives, or by blending three biopolymers, such as CS, Gelatin, and PVA, to make a ternary blend, which has been widely used in the preparation of packaging materials with good physical and chemical properties[10].

Nanoparticles have been used as potential food preservative agents in active food packaging, such as Zinc oxide nanoparticles, which act as antimicrobial and antioxidant agents. The incorporation of ZnO-NPs into chitosan films enhances their antimicrobial and antioxidant properties [11]. Recently, antibacterial films have been used in multiple applications; in the food industry, life sciences, and medical services [12]. Active compounds like essential oils can be incorporated into biodegradable polymer films to improve their functional properties, such as antimicrobial properties [13]. In particular, edible films combining hydrophilic and hydrophobic ingredients could retard moisture loss and gas migration and ensure food integrity, reducing the necessity of using synthetic plastics [14].

Lemongrass grows in almost all tropical and subtropical countries [15] and exhibits antimicrobial activities against a broad range of bacteria, including *Campylobacter jejuni*, Listeria monocytogenes, *Escherichia coli* O157, *Staphylococcus aureus* and *Bacillus cereus* [16] and yeast and fungi [17,18] However, direct incorporation of EOs in the coating or films considerably weakens the mechanical properties of the coating or film, decreases the EOs loading capability and worsens the risk of oiling off the Eos [19]. However, using nanoemulsions in coating-forming solutions has additional advantages, including improved film homogeneity, increased antimicrobial activity, decreased compound dosage, reduced interactions with other food matrix components, increased stability of the compounds under stress, and reduction mass transport of the compounds through coating [20]. Additionally, Lemongrass nanoemulsion demonstrated antimicrobial activities against various pathogens superior to free lemongrass oil [21]. US Food and Drug Administration categorized Chitosan, ZnO-NPs, TA, and plant essential oils as GRAS [22-25], as well as PVA, which can be used as a covering material for various foods without raising any health concerns [26].

Hence, the main objective of this work was to prepare a ternary blend of chitosan (CS), polyvinyl alcohol (PVA), and gelatin (GE) that have significant characteristics to overcome any drawbacks facing the food packaging materials. Furthermore, to investigate the effect of incorporation of lemon grass nanoemulsion and/or ZnO-NPs within the nanocomposite on the films´ characteristics (mechanical properties, thermal properties, barrier properties "water vapor and gas permeability", and hydrophobicity) on extending the shelf life of chilled chicken

meat, and on the population of Listeria monocytogenes and *Salmonella Typhimurium* in the chilled chicken meat.

2. Materials and Methods

2.1. Materials.

Chitosan (CS) of average molecular weight Mv = 92,700 g mol^{-1} and degree of deacetylation of 82.5%, glacial acetic acid (HAc), polyvinyl alcohol (PVA), gelatin (GE) from bovine skin type B, zinc-acetate (Zn $(CH_3COO)_2.2H_2O$), tween 80, glycerol, thiobarbituric acid (TBA), butylated hydroxyanisole (BHA), and 1, 1, 3, 3-tetraethoxypropane (TEP) were obtained from Siga-Aldrich Chemicals (Cairo, Egypt). Sodium hydroxide (NaOH) was obtained from Acros. Standard plate count agar "SPC" (TM MEDIA), Sabaroud's dextrose agar (Biolab), sodium chloride "NaCl" (ADWIC), Oxford medium base "OMB" (HIMEDIA), Xylose Lysine Desoxycholate "XLD" (HIMEDIA), tryptic soya broth (BIOMARK), nutrient agar (HIMEDIA), nutrient broth (LAB M) , Mueller Hinton broth "MHB" (TM MEDIA), and Mueller Hinton Agar "MHA" (OXOID). Listeria Selective Supplement (Oxford formulation, SR0206). Tannic acid (TA), standard buffer solutions at pH 4.0, pH 7.0, and pH 10.0, Trichloroacetic acid (TCA), and absolute ethanol, all chemicals used were at least of analytical grade. Lemon grass essential oil was obtained from the National Research Centre, Cairo, Egypt, and stored at 4 °C till further use.

2.2. Methods.

2.2.1. Preparation of ZnO nanoparticles (ZnO-NPs).

Zinc oxide nanoparticles were prepared using a hydrothermal method in an alcoholic medium via the reaction of zinc acetate (Zn $(CH_3COO)_2.2H_2O$) and sodium hydroxide (NaOH) as a base. In the current work, 1.97g Zn $(CH_3COO)_2.2H_2O$ and 0.72g NaOH were dissolved in 500 mL of absolute ethanol, and the reaction was refluxed at 70 °C for 3 h. The (CH_3COO) group reacted with sodium hydroxide and changed the zinc acetate into ZnO. Subsequently, the ZnO was dispersed in an ethanol medium and mixed with DI water for purification. ZnO-NPs were then separated from the dispersion supernatant by centrifugation at 7000 rpm for 5 min repeatedly. Finally, the ZnO nanoparticles were dried in an electric oven to obtain ZnO-NPs. TEM result indicated that the size of ZnO nanoparticles was in nanoform.

2.2.2. Pathogenic strains.

The tested reference bacteria, *L. monocytogenes* (NCTC 13372\ATCC® 7644) and *Salmonella Typhimurium* (NCTC 12023\ATCC® 14028), were obtained from the certified food lab at the Animal Health Research Institute (AHRI), Dokki, Egypt. All strains were maintained as frozen stocks in Tryptic soya broth (TSB) supplemented with 10% glycerol.

2.2.3. Preparation of bacterial suspension.

Stock cultures were subcultured in tryptic soy broth twice (incubated at 35 °C for 24 h) before use. A loopful from the subcultured reference strains were streaked over non-selective media (nutrient agar) several times to ensure their purity, then streaked onto selective media, Oxford medium base supplemented with oxford supplement for *Listeria monocytogenes* and

xylose lysine deoxycholate agar for *Salmonella Typhimurium*, and held at 37 °C for 48 h. About 2-4 pure colonies of each bacterial strain were inoculated into 5 mL tryptic soy broth. The cultured bacterial strains were serially diluted (double fold) with sterile normal saline solution, and the suspensions were compared to freshly prepared and vortexed 0.5 McFarland standards against a white background with black lines (i.e., a Wickerham card) to assess the required bacterial concentration [27].

2.2.4. Preparation of lemon grass nanoemulsion (Lg-NE).

Tween 80 was added to double-distilled water (2 v/v%) at room temperature with continuous stirring using a magnetic stirrer for 10 min until a clear homogeneous solution was obtained. The lemon grass was added slowly, drop by drop, at a rate of 1 drop/min, with continuous stirring for 15-20 mins. The resulting crude emulsion was sonicated using a bath sonicator, Ultrasonic Cleaner (Model 104X, 230V, 50/60 Hz, max power: 715 watt, DENSPLY CERAMCO). Sonication was continued for 1 h in all cases. Ultrasonication produces intensive and disruptive forces that help minimize lemon grass nanoemulsion droplets [28].

2.2.5. Determination of the minimum inhibitory concentration (MIC) and minimum lethal concentration (MLC).

According to the broth dilution method, the minimum inhibitory concentration and minimum lethal concentration were determined for the raw lemon grass and its nanoemulsion against the tested strains, *L. monocytogenes*, and *Salmonella Typhimurium*, according to [29], with some modification. The cultures used in the test were adjusted to 5×10^{7}CFU/mL with the aid of 0.5 McFarland standard turbidity (5×10^{8} CFU/mL). As well, different oil concentrations were prepared to assess the MIC and MLC for pure oil (5, 2.5, 1.25, 0.625, 0.312, 0.156, and 0.078% for *Salmonella Typhimurium* and 0.5, 0.25, 0.125, 0.0625, and 0.031% for *L. monocytogenes*). Additionally, 0.5% v/v sterile tween 80 was added to the medium to enhance the solubility of the pure oil in aqueous solutions. Furthermore, lemongrass nanoemulsion concentrations (0.5, 0.25, 0.125, 0.0625, 0.031, and 0.015%) were prepared to test both bacterial species. 100 μl of +ve bacterial culture was added to each prepared concentration. Positive control was prepared for only the bacteria in the MHB, while the negative control included only the oil or the nanoemulsion in the MHB. Inoculated media were incubated at 37ºC for 24 h, and the MIC was determined as the lowest concentration of an additive that demonstrated no visible growth. For MLC determination, 100 µL of the media without obvious growth were cultured onto Mueller Hinton Agar (MHA) and incubated for 24 h at 37ºC. MLC is defined as the lowest concentration that could kill 99.9% of the bacterial population.

2.2.6. Preparation of bionanocomposite films.

Chitosan solution (CS) 3% (w/v) was prepared in 100 mL of 2% v/v acetic acid solution with stirring (8 h at 70 °C). Simultaneously, aqueous solutions of polyvinyl alcohol (PVA) (5% w/v) and Gelatin (GE) (3% w/v) were prepared separately with continuous stirring at 70°C for 6 h and at 50ºC for 2 h, respectively. CS/PVA/GE ternary blend was obtained by mixing the three previously prepared polymer solutions at the ratio of 60:30:10% (v/v). Then glycerol (30% from the weight of the total solids of the polymers) was added steadily under constant stirring, afterward, the tannic acid (at a percent of 5% from hard solids of the polymers). The

CS/PVA/GE/ZnO bionanocomposites ternary blend was fabricated by adding zinc oxide nanoparticles (2% of the weight of the film's dry matter). Bionanocomposites with different loadings of the Lemongrass nanoemulsion (Lg-NE) (13.8, 20, and 25 % v/w) were prepared by adding Lg-NE to the previous blend solutions during stirring and adjusting the mixture pH by using NaOH solution (0.1 N). With the same procedures, blank films (CS/PVA/GE blend and CS/PVA/GE/ZnO bionanocomposites) were also prepared. After adjusting the pH, the solutions were left under magnetic stirring for 5 h and were maintained at room temperature for 24 h to eliminate air bubbles formed during stirring.

The homogeneous bionanocomposite suspensions (200 mL) were poured onto transparent glass rectangular Petri dishes (33.5×23.8 cm) and left undisturbed at room temperature for 72 h to evaporate the solvent mold the films. The formed bionanocomposite films were peeled off the mold using a spatula and stored in a desiccator before characterization. The recipe of CS/PVA/GE blend and CS/PVA/GE/ZnO bionanocomposites containing different ratios of Lemon grass nanoemulsion are shown in (Table 1).

Table 1. Recipe of CS/PVA/GE blend and CS/PVA/GE/ZnO bionanocomposites containing different ratios of Lg-NE.

Symbol	Film name	ZnO-NPs, %	Lg-NE, %
(T. H)	CS/PVA/GE blend	0.0%	0.0%
(T.G)	CS/PVA/GE/ZnO bionanocomposites	2%	0.0%
(T. F)	CS/PVA/GE/ Lg-NE	0.0%	13.8%
(T. E)	CS/PVA/GE/ Lg-NE	0.0%	25%
(T. D)	CS/PVA/GE/ZnO/Lg bionanocomposites	2%	6.9%
(T. C)	CS/PVA/GE/ZnO/Lg bionanocomposites	2%	13.8%
(T. B)	CS/PVA/GE/ZnO/Lg bionanocomposites	2%	20%
(T. A)	CS/PVA/GE/ZnO/Lg bionanocomposites	2%	25%

Polyethylene bags were also used for packaging samples without a bionanocomposite film as a negative control (T.I).

2.3. Characterization.

2.3.1. Droplet size determination.

The droplet size of the prepared emulsion was measured using dynamic light scattering (DLS) with a Nano Zetasizer laser diffractometer (Malvern Instruments Ltd, Worcestershire, UK) equipped with a backscatter detector (173º), which is applicable to measure submicron particles and set at 633 nm at 25°C.

2.3.2. Morphological evaluation.

Morphological analysis of nanoemulsions and ZnO-NPs was performed by Transmission Electron Microscopy (TEM). Initially, the prepared nanoemulsion was diluted (1:10 v/v in water), followed by dripping it in a sample grid. After passing 1 min, the samples were dried with a paper film and stained with uranyl acetate (2%). They were kept in a vacuum desiccator and observed by TEM at 80 KV (JEM-1200 EXII, JEOL, Japan). Also, scanning electron microscopy (SEM) (High-Resolution Quanta FEG 250-SEM, Czech Republic) has been used to assess the morphology of the prepared nanocomposites. The sample surfaces were evaluated at low vacuum and without coated gold.

2.3.3. Infrared (IR) spectral analysis.

FT-IR spectra of the fabricated samples were carried out using the KBr method using a Mattson 5000 spectrometer (Unicam, UK).

2.3.4. X-ray diffraction (XRD).

Using a Philips X-ray diffractometer (PW 1930 generator, PW 1820 goniometer) and Cu K radiation (45 kV, 40 mA, with $\lambda = 0.15418$ nm), the crystal structure of the filler powders was determined. The analysis's scans were conducted in a two-dimensional (2D) range of 5 to 80^{o} with a step size of 0.02 and a step time of 1s.

2.3.5. Permeability of the fabricated bionanocomposites film.

GBI W303 (B) Water Vapor Permeability Analyzer (China) was used to measure the Water vapor transmission rate (WVTR) using the cupping technique. The water vapor permeability of the tested film was determined by the amount of water vapor that could pass through it. WVTR was additionally determined using the following criteria as the mass of water vapor moved over a unit area in a unit time at a controlled temperature (38^{o}C) and humidity (4%) (TAPPI T464, ASTM D1653, DIN 531221, ISO 2528). Furthermore, the oxygen transmission rate (OTR) was evaluated by N530 Gas Permeability Analyzer (China), using (ISO2556-2001) as an international standard.

2.3.6. Mechanical properties evaluations.

Using a universal testing machine (Hants, UK) equipped with a 5 kN load cell and operating on the samples at a rate of 5 mm/min, the mechanical characteristics of the generated bionanocomposite films were evaluated in accordance with the ASTM D638-91 standard.

2.3.7. Contact angle examinations of the prepared bionanocomposites.

Data Physics Instruments GbH, Filderstadt, Germany, employed an OCA20-programmed and software-controlled video-based contact angle meter to determine the dynamic contact angle of a distilled water drop on the synthesized bionanocomposite and on the mixture. These observations were made at 25 °C and 58% relative humidity.

2.3.8. Thermogravimetric analysis (TGA).

Using the Netzsch DSC-200PC analyzer (Germany), the thermal stability assessment was completed. The samples were heated from 25°C to 600^{o}C at the rate of 10^{o}C/ min in a nitrogen environment. Sample weight loss was calculated as a function of temperature.

2.3.9. Gel swelling property.

The test film samples were dried at 37^{o}C for 12h in an incubator and then precisely weighed. After that, about 1 g of the dried film was immersed in distilled water, about 10 mL, for 1–8 h. Afterward, remove the films from the water and try removing the surface water using filter paper through gentle blotting, followed by immediately weighing the films to obtain the wet weight. The following equation was used to determine the films' capacity to absorb water or to swell:

$$S = \frac{W_S - W_d}{W_d} \times 100$$

where Ws and Wd are the weights of the samples in the swollen and dry conditions, respectively, and S is the percentage of water absorption of the films at equilibrium.

2.3.10. Release of the Lemon grass essential oil from the nanocomposite film.

Raw lemongrass essential oil (Lg-EO) double fold serial dilution (50%-0.0015%) was prepared in food simulant solution (50% Ethanol:50% distilled water), and used to obtain a calibration curve correlating the absorbance at 376 nm to the essential oil concentration. The ideal wavelength for measurement of the oil concentrations was previously obtained through spectroscan to get the highest absorbance peak intensity. The used solvent is a standard simulant for migration studies, according to [30].

Sustained release of the Lg-NE from the structure of CS/PVA/GE/ZnO/Lg bionanocomposites in food simulants (50:50 Ethanol: Distilled water) was measured using the dialysis method [31] with modification. Bionanocomposites with specific dimensions (2×2 cm^2) were introduced within the dialysis bag and suspended in 2 mL of the food simulants to perform the release studies. The release kinetic of the essential oil nanoemulsion from these structures was measured for 286 h. The trial was done under refrigeration at 4°C and under static conditions (no agitation). At different intervals (0, 0.5,1, 1.5, 2, 2.5, 3, 3.5, 4, 5, 6, 7, 8, 9, 10, 12, 18, and 24 h., then every 12 h. till the end of the test). Each time 1 mL of the medium was withdrawn, the removed volume was replaced with 1 mL of the corresponding fresh food simulant. The absorbance of each sample (removed volume) was measured at 376 nm using a UV–VIS spectrophotometer (Thermo Scientific Evolution 300 UV-Vis, England) and converted to the concentration of the nanoemulsion released using the equation of the calibration curve. The cumulative release of the nanoemulsion was calculated by sequentially adding the released concentration after each step and was drawn against the time into the cumulative release curve according to [32].

2.3.11. Application of nanocomposite films for evaluating their physicochemical and microbiological effects.

Figure 1 illustrates the application of nanocomposite films onto the chilled poultry meat parts (breasts and thighs), as they were obtained from the retail markets in Assiut city, Egypt, and immediately transferred to the laboratory in sterilized plastic bags under complete hygienic and refrigeration conditions (4±1°C).

In the laboratory, under complete aseptic conditions, the purchased samples were divided into two sets (treatment and control groups):

Treatment groups include packaging with prepared films; (T. A), (T. B), (T. C), (T. D), (T. E), and (T. F).

Control groups, those packaged with CS/PVA/GE/ZnO bionanocomposites (T. G) and CS/PVA/GE blend (T. H) films (Blank films), beside those packed in sterilized polyethylene plastic bags (T. I).

The entire sample (breast and thigh) was wrapped by the prepared film from all sides, then placed in foam plates (sterilized by UV lamp for 20 min) and covered with ethanol-sterilized stretch plastic. Samples were then stored in a refrigerator (4°C) throughout the trial till sensory spoilage. Samples were harvested at specific time intervals of 0 time (the time of packaging) and after 24 h, 3, 5, and 7 days (appearance of spoilage signs) for physicochemical

and microbiological analysis. Control samples were handled with the same procedure and at the same intervals.

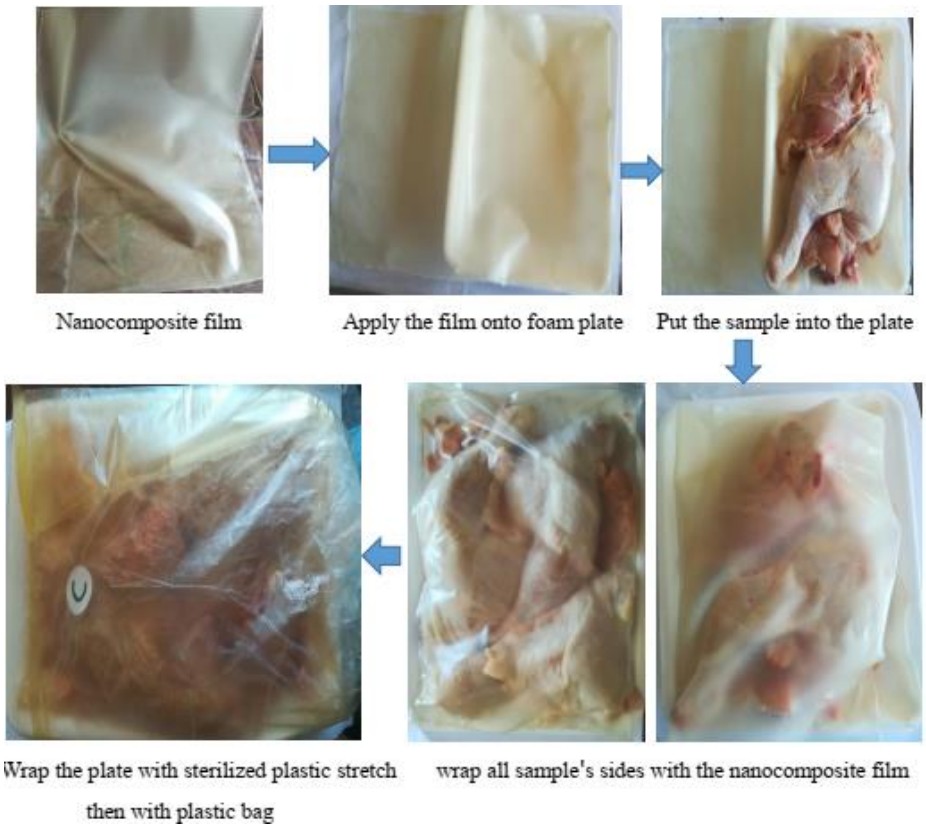

Figure 1. Application of the nanocomposite films onto chicken meat parts for quality evaluation.

The reduction (R) percentages were calculated according to the following equation:

$$R\% = \frac{(\text{count of the treatment at 0 time} - \text{count of the same treatment at specific time})}{\text{count of this treatment at 0 time}} \times 100$$

2.3.12. Physicochemical evaluation of meat samples.

2.3.12.1. Sensory evaluation.

Eight panelists selected from the staff of the Food Hygiene Department, Faculty of Veterinary Medicine, Assuit University, aged 25–30, who were previously trained to perform the sensory evaluations of both the treated carcasses, and the controls based on the appearance, viscosity, flexibility, and flavor of the meat as demonstrated in Table 2. The sensory scores were ranked from 1 to 5, with 5 as the highest and 1 as the lowest score [33]:

Table 2. Sensory evaluation standards for chilled poultry meat.

Color and luster	Viscosity of appearance	Flexible	Flavor	Score
Bright pink and shiny	Wet and not sticky	Recovering immediately	The freshness smell	5
Pink and a little shiny	A little wet and not sticky	Recovering a bit slowly	No abnormal odor	4
Red and dull	Non-wet and sticky	Recovering slowly	A little off-flavor	3
Red and dull	A little dryness and sticky	Recovering very slowly, even unrecoverable	Sour	2
Deep red and dull	Dryness and sticky	Recovering very slowly, even unrecoverable	Sour heavily	1

2.3.12.2. Determination of pH.

Using a pH meter (AD1030, Adwa Instruments, Woonsocket, RI, USA), pH values were evaluated according to Takma and Korel [2].

2.3.12.3. Determination of Thiobarbituric Acid Reactive Substances (TBARS).

TBARS were determined as described by Buege and Aust [34].

2.3.13. Microbiological quality of chicken meat samples.

Chicken meat samples (10 g) were homogenized with 90 mL of sterile saline solution (0.9% NaCl w/v) using a stomacher (Seward 400) at room temperature for 3 min. The obtained mixture was serially diluted (tenfold) in 0.9% NaCl sterile saline solution. Yeast and mold were counted according to Hungerford *et al*. [35].

2.3.14. Challenge study: Effect of the prepared bionanocomposites on Listeria monocytogenes and *Salmonella Typhimurium*.

According to Morsy *et al*. [36], as demonstrated in (Figure 2), chicken meat samples were cut into cubes 5×5×1 cm with sterile scalpels and tweezers under complete aseptic conditions. The samples were surface treated with ultraviolet light (UV) for 20 min on each side to reduce background microflora [37]. Meat cubes were aseptically inoculated overnight and diluted cultures of *L. monocytogenes* or *S. Typhimurium* with shaking for 10 min to ensure an even distribution of the bacterial suspension. Bacterial cultures were diluted in a 0.9% saline solution, obtaining a concentration between 10^4: 10^5 CFU/mL for S. Typhimurium and approximately 10^7 cfu/mL for *L. monocytogenes*, comparing the inoculum with 0.5 Mac Farland scale for each bacterium' [29].

Inoculated samples were then placed in sterile Petri dishes, immersed in the bacterial suspension, and kept in the refrigerator for 20 min. After that, the samples were left to drip the excess suspension for 10 mins at room temperature. Inoculated chicken meat cubes were wrapped with the designated films previously sterilized by ultraviolet light (UV) for 30 min on each side. Wrapped samples for each treatment were immediately packed into sterile plastic stretches and sterile polyethylene bags to avoid contamination, then stored under refrigerated conditions (4 ± 1 ◦C). All treatments were tested for inoculum count till they became organoleptically unacceptable. Controls include inoculated samples, covered with the blank film without LGEO and others only packed in sterile polyethylene bags, submitted to the same procedures as other treatments.

On days 0, 1, 3, 5, 7, 10, and 12, samples were analyzed for population count. At each sampling time, the package was opened, and 10 g of each sample was transferred aseptically to a stomacher bag with 90 mL of 0.9% NaCl sterile saline solution and homogenized for 2 min (Seward 400 Stomacher). Ten-fold serial dilutions were made in sterile saline solution, and 100 µL of the homogenate was plated in duplicate onto Modified Oxford Agar for *L. monocytogenes* and Xylose Lysine Deoxycholate Agar for *S. Typhimurium* to determine the count. Inoculated bacteria were counted after 1 to 2 days of incubation at 37 °C. Population count was expressed as $\log_{10}$ CFU/g [38,39]. The reduction (R) percentages were calculated according to the following equation:

$$R\% = \frac{(\text{count of the treatment at 0 time} - \text{count of the same treatment at specific time})}{\text{count of this treatment at 0 time}} \times 100$$

The author's institute's policy on animal usage and ethics was followed when conducting studies; details on compliance with local, national, and international laws or regulations were provided when possible. (Medical Research Ethics Committee (MREC) Decision No: 20177.

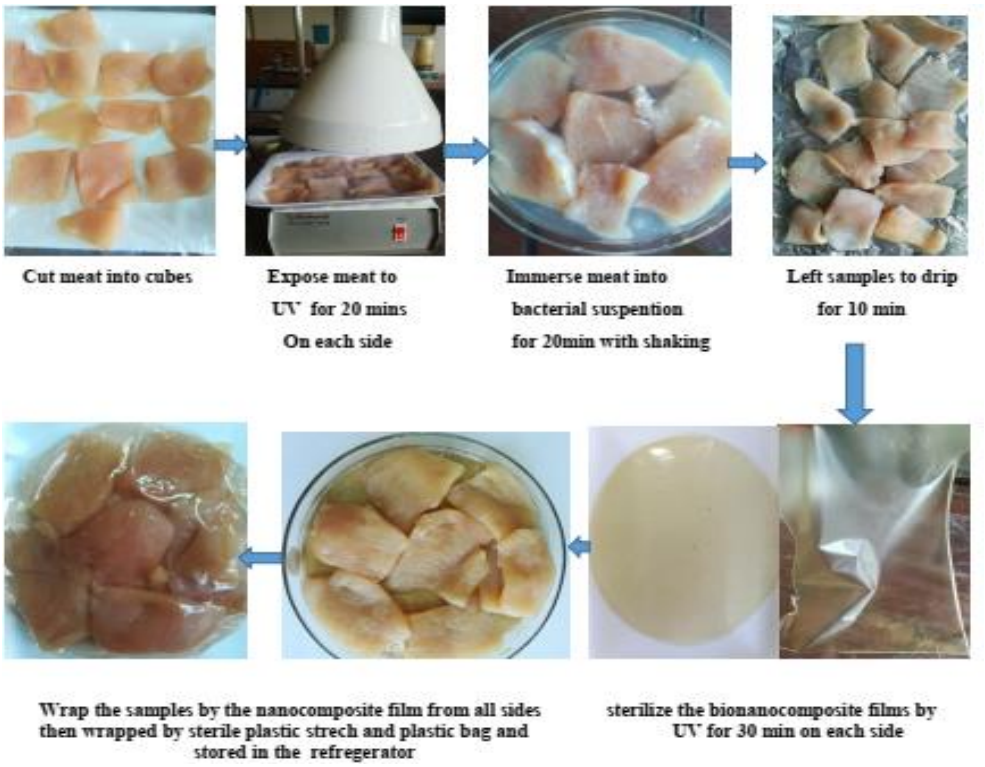

Figure 2. Procedures of Challenge study.

3. Results and Discussion

3.1. Evaluation of the prepared ZnO-NPs and Lg-NE

In the current work, zinc oxide nanoparticle was prepared using a hydrothermal method. The morphology of the fabricated ZnO nanoparticles was assessed using a transmission electron microscope (TEM) (Figure 3a). The transmission electron microscope image of ZnO-NPs displayed that the zinc oxide particles develop slowly and create hexagonal constructions besides gathering identical bullets as well as chief of the fabricated zinc oxide nanoparticles existing in a cubic structure. Furthermore, the TEM images of the prepared ZnO-NPs were a cubic structure that is established via XRD pattern, while Kumar *et al*. [40] found that the TEM images of most green synthesized ZnO-NPs were polyhedral in shape. Moreover, the TEM of the prepared Lemon grass nanoemulsion (Lg-NE) was obtainable in (Figure 3b).

The dynamic light scattering effect on the particle size examination of the prepared ZnO-NPs was revealed in (Figure 3c) which showed the particle size is around 335 nm. Furthermore, the drop size of the fabricated Lg-NE was obtainable in (Figure 3d), which showed an average diameter of about 380 nm, distinguishing the particle size of lemon grass at the nano level throughout the solubilization of Lg in water.

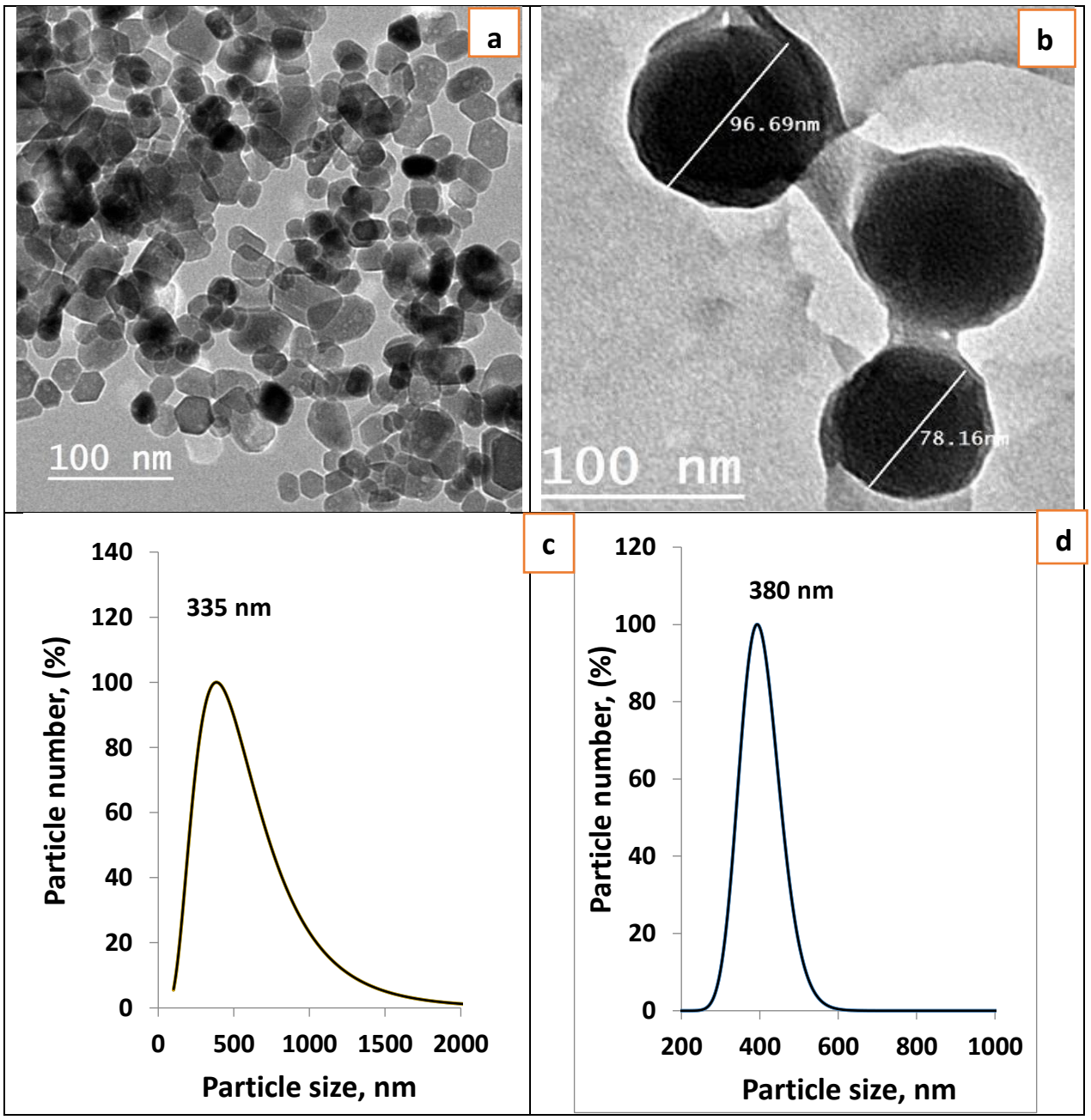

Figure 3. (a) TEM image of ZnO-NPs; **(b)** TEM image of Lg-NE; **(c)** Particle size of ZnO-NPs; **(d)** Particle size of Lg-NE.

3.2. Structural properties of ZnO-NPs as well as its bionanocomposites.

The structure of the prepared ZnO-NPs and CS/PVA/GE/ZnO/Lg-NE bionanocomposites was evaluated using the XRD pattern method, which utilizes to determine the crystal structure. Figure 4a shows the X-ray diffraction pattern of the fabricated ZnO-NPs with Lemon grass nanoemulsion (Lg-NE); all peaks associated with ZnO nanoparticles seemed in the XRD pattern, while some peaks correlated to the existence of Lg-NE. ZnO-NPs prepared using the hydrothermal method demonstrated diffraction peaks at 31.49, 34.28, 35.92, 46.56, 56.02, 61.8, 66.91, and 68.56º of 2Ɵ. All the ZnO nanoparticles diffraction bands connected to the crystal planes (100), (002), (101), (102), (110), (103), (200), and (112), as presented in (Figure 4a). The ZnO-NPs average crystallite size was evaluated from the width of main peaks via the Scherrer equation, and they were around ~20 nm. The synthesized ZnO-NPs were confirmed through the TEM image. Moreover, the XRD of chitosan shows the main peak, at

18.33° resulting from the crystalline phase, which was associated with the reflections (200). Furthermore, a broad area under this peak extending from around 10° to 70° is associated with the major amorphous phase. Additionally, the XRD of CS/PVA/GE displays four peaks characteristic of polymer crystallinity at 16.88° (strong), 13.84° (medium), 18.01(weak), and 24.43° (weak).

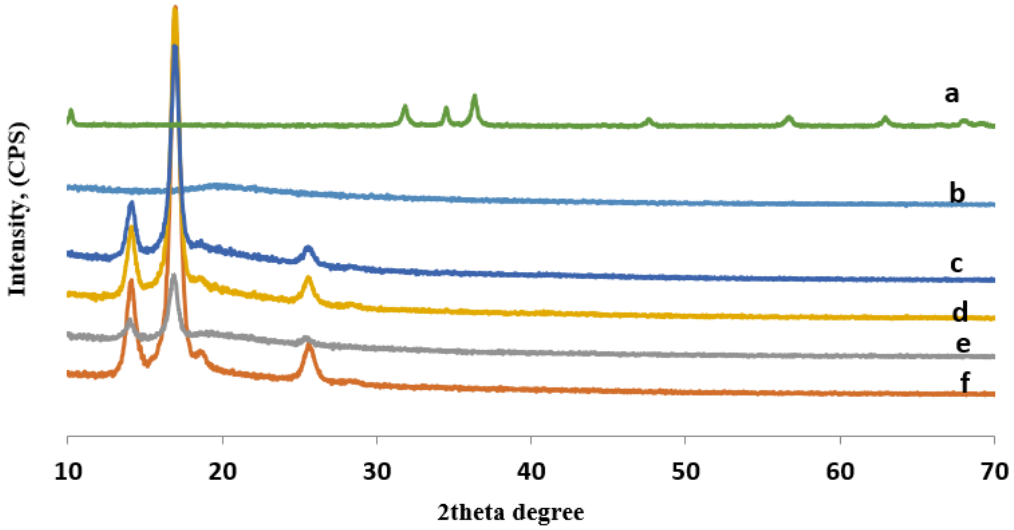

Figure 4. XRD pattern of **(a)** ZnO-NPs; **(b)** CS; **(c)** CS/PVA/GE blend, as well as CS/PVA/GE/ZnO/Lg-NE bionanocomposites containing different concentrations of Lg-NE; **(d)**13.8 %; **(e)** 20%; **(f)** 25%.

Additionally, the XRD pattern of CS/PVA/GE/ZnO/Lg-NE bionanocomposites loaded by 2% of ZnO-NPs and different ratios of Lg-NE (13.8, 20, and 25%) were demonstrated in (Fig. 4 c, d, and e) where the characteristic peaks of chitosan, PVA and GE matrix appear in the formed bionanocomposites films. Soltanzadeh *et al*. [41] demonstrated that XRD of chitosan nanoparticles loaded by lemongrass essential oil (LGEO) exhibited a broad high-intensity peak at 2θ = 19–25° inferring the entrapment of LGEO within CSNPs compared to non-loaded CSNPs. In addition, the peak intensity related to the addition of ZnO nanoparticles in the bionanocomposites matrix was very slight owing to the very few ratios of ZnO-NPs, which are supplementary to the bionanocomposite films. The crystal structure could also develop the barrier and mechanical properties of the fabricated CS/PVA/GE/ZnO/Lg-NE bionanocomposites films.

3.3. FT-IR investigation of the synthesized CS/PVA/GE/ZnO/Lg bionanocomposites.

The synthesized CS/PVA/GE blend, CS/PVA/GE/ZnO, and CS/PVA/GE/ZnO/Lg bionanocomposites, each containing a different loading of Lg-NE, all were investigated through FT-IR (Figure 5). Chitosan's spectra exhibit peaks at 856 and 1055 cm^{-1}, which are consistent with its saccharide structure [42]. Nevertheless, there were substantial absorption peaks at 1651 and 1344 cm^{-1}, which are characteristic of chitosan and have been classified as amide I and III peaks, respectively, despite many peaks accumulating in the amide II peak region from 1641 to 1670 cm^{-1}. The CH_3 symmetrical deformation mode was connected to the strong peaks at 1313 and 1444 cm^{-1}. The broad peak at 1043 cm^{-1} represents the chitosan C-O stretching vibration. The typical C-H stretch vibration peaks are 2912 and 2952 cm^{-1} [43].

The FT-IR spectrum of pure PVA is also displayed in Figure 5, where all major peaks associated with the hydroxyl and acetate groups were found. Furthermore, the stretching OH from the intramolecular and intermolecular hydrogen bonds is correlated with the broadband

seen between 3580 and 3150 cm^{-1}. The stretching of C-H from alkyl groups is responsible for the vibrational band seen between 2860 and 3986 cm^{-1}, while the peaks between 1740 and 1720 cm^{-1} are associated with the stretching of C-O and C-O from the acetate group from PVA (saponification action of polyvinyl acetate) [44]. FT-IR absorption bands at 3318 and 2915 cm^{-1}, which correspond to OH stretching and CH_2 asymmetric stretches from PVA, are also visible in the IR spectra of the CS-PVA blend. The amides I and III of C-O stretching vibration, N-H bending of NH_2, and CH_2 twitching linked with the OH group from CS are responsible for the peaks at 1664, 1570, and 1331 cm^{-1}. OH, and CH group changes are believed to be responsible for the peak at 1417 cm^{-1}. A high peak was seen at about 3340 cm^{-1} for the CS/PVA/GE/ZnO/Lg bionanocomposites film, which contains 2% ZnO-NPs and different loadings of Lemon grass nanoemulsion (Lg-NE). These overlapping absorption bands reflect O-H vibrations and N-H stretching. Additionally, symmetric and asymmetric C-H vibrations can be distinguished by the bands at 2910–2840 cm^{-1}. The amide I + amide II groups are responsible for the apparent absorption peaks that emerge around 1623 and 1553 cm^{-1}, respectively.

Furthermore, C-O stretching vibration is mainly responsible for the band at 1022 cm^{-1}. These observations show that the addition of ZnO nanocomposites improved the hydrogen bonding in the CS/PVA/GE/ZnO/Lg bionanocomposite films, which may be the cause of the better mechanical properties of the produced CS/PVA/GE/ZnO/Lg bionanocomposite films.

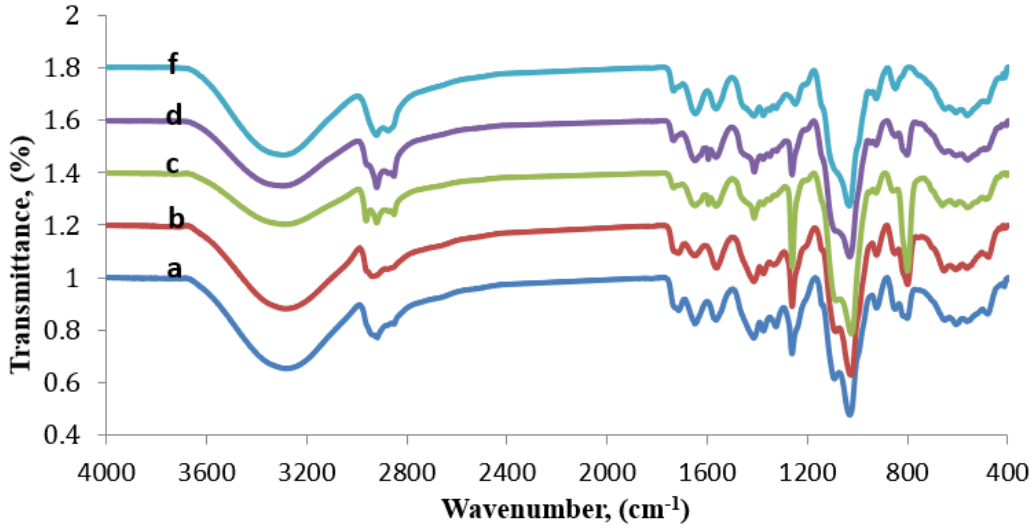

Figure 5. FTIR of **(a)** CS/PVA/GE blend; **(b)** CS/PVA/GE/ZnO bionanocomposites as well as CS/PVA/GE/ZnO/Lg bionanocomposites containing different concentrations of Lg-NE; **(c)** 13.8 %; **(d)** 20%; **(e)** 25%.

3.4. Morphological evaluation of the prepared CS/PVA/GE/ZnO/Lg bionanocomposite films.

Figure 6 displays the morphology of the prepared CS/PVA/GE/ZnO/Lg bionanocomposite films containing 2 % ZnO-NPs and different ratios of lemon grass nanoemulsion (Lg-NE), which SEM evaluated. Figure 6a shows The SEM images of CS/PVA/GE blend where the surface of a ternary blend of chitosan, poly (vinyl alcohol), and gelatin was comparatively smooth, representative of desired compatible bionanocomposites as shown in (Figure 6a). Nevertheless, by adding 2% ZnO-NPs and different ratios of lemon grass nanoemulsion (Lg-NE) to the CS/PVA/GE blend, significant modifications in the fabricated CS/PVA/GE/ZnO/Lg bionanocomposite film morphology, making the film surface to become rough as recognized in (Figures 6 b, c, and d). Conversely, incorporating 2% and 4% ZnO-NPs

into chitosan-gelatin nanocomposite revealed a smooth, compact, and heterogeneous surface morphology compared to the control films without ZnO-NPs [40].

Furthermore, by raising the concentrations of Lg-NE into the bionanocomposite matrix, the compatibility between the three-biopolymer increased, and the Lg-NE incorporated into the polymer chains in the presence of ZnO-NPs, which leads to improved permeability, mechanical and thermal properties of the prepared CS/PVA/GE/ZnO/Lg-NE bionanocomposite.

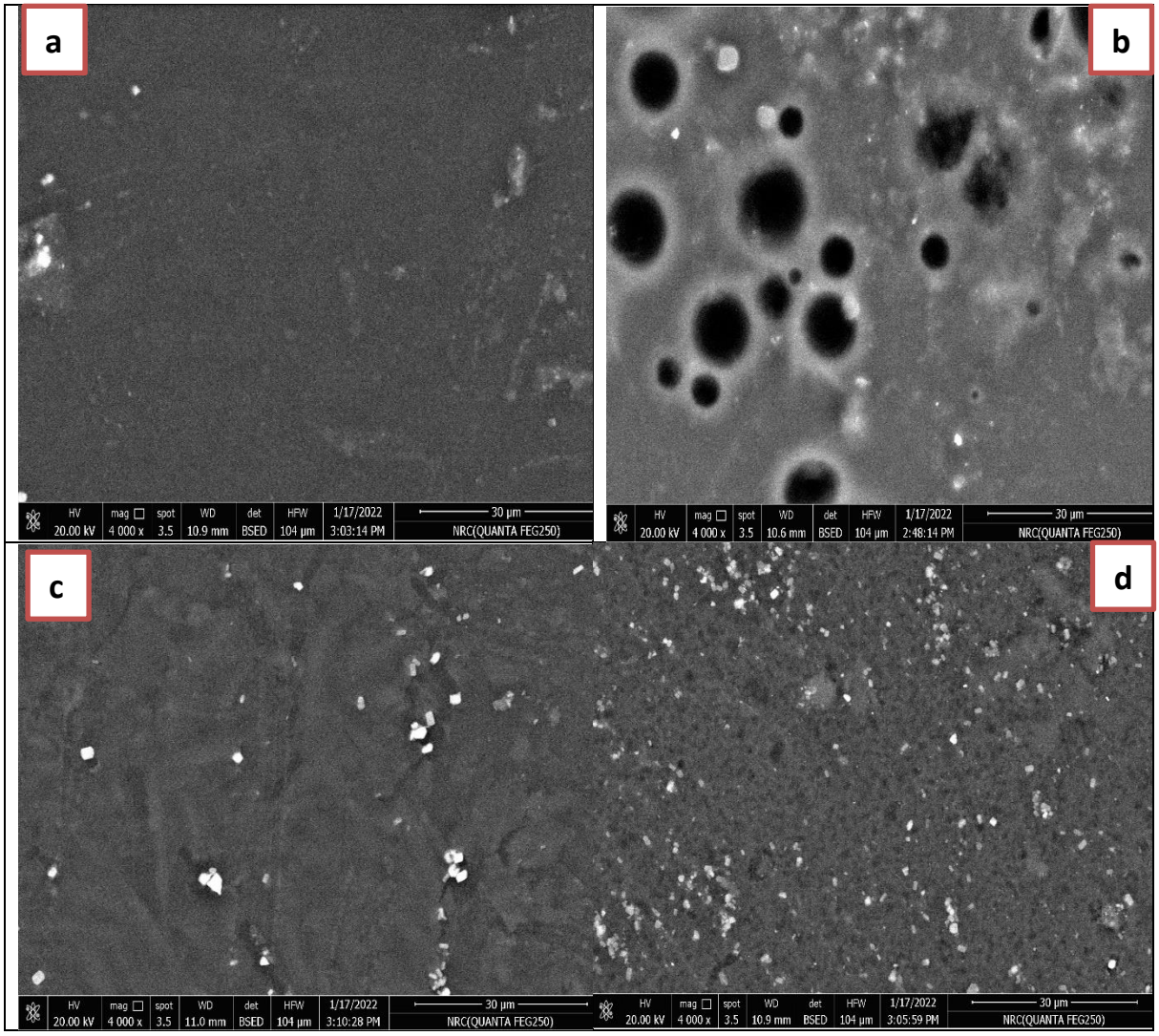

Figure 6. SEM image of **(a)** CS/PVA/GE blend, as well as CS/PVA/GE/ZnO/Lg bionanocomposites containing different concentrations of Lg-NE; **(b)** 13.8 %; **(c)** 20%; **(d)** 25%.

3.5. The permeability evaluation of the prepared CS/PVA/GE/ZnO/Lg bionanocomposites

The water vapor transmission rate (WVTR) and the oxygen transmission rate (OTR) of the fabricated CS/PVA/GE blend, as well as CS/PVA/GE/ZnO/Lg bionanocomposites films, were studied using a water vapor permeability analyzer and GBI W303 (B) and N530 gas permeability analyzer, respectively. It is famous that the water vapor and oxygen permeability are substantial for promising the applicability of materials used for packaging applications, particularly in foodstuff packaging. Therefore, the prevailing quantities of water vapor in oxygen gas from the surrounding atmosphere into the food or fatalities from the food to the surrounding atmosphere apply distinguished influence on the food from the constancy point and the quality during the protection and the time of shelf-life. Table 3 shows the OTR and WVTR of the fabricated CS/PVA/GE blend, as well as CS/PVA/GE/ZnO/Lg

bionanocomposites. The obtained results from (Table 3) demonstrated that CS/PVA/GE blend in the absence of ZnO-NPs and Lg-NE, which reveals greater WVTR compared with CS/PVA/GE/ZnO and CS/PVA/GE/ZnO/Lg bionanocomposites, by adding 2% of ZnO-NPs to the CS/PVA/GE blend the WVTR decrease from 2119.87 to 2013.56 g/(m^2.day). Also, by adding different concentrations of Lg-NE into the prepared CS/PVA/GE/ZnO/Lg bionanocomposites in the presence of 2% ZnO-NPs the WVTR declined from 2013.56 g/(m^2.day) to 1986.20, 1848.31, and 1622.38 g/(m^2.day), when using different loadings of Lg-NE (13.8 %, 20%, and 25%), respectively.

Furthermore, the OTR is essential for the basic material for oxidation procedures, which is responsible for changes in food flavor, odor, color, and nutrient worsening. Therefore, CS/PVA/GE/ZnO/Lg bionanocomposites films that offer appropriate O_2 barriers might assist in emerging food shelf-life extension and food quality. By adding 2% ZnO-NPs and various ratios of Lg-NE, the oxygen transmission rate (OTR) of the prepared CS/PVA/GE/ZnO/Lg bionanocomposites films was emphasized. Moreover, The OTR of the fabricated CS/PVA/GE/ZnO/Lg bionanocomposites was increased by higher loadings of different ratios of Lg-NE and 2% ZnO-NPs in the CS/PVA/GE blend. Thus, the OTR of the fabricated CS/PVA/GE/ZnO/Lg bionanocomposites films affectedly improved with adding of Lemon grass nanoemulsion (13.8%, 20%, and 25%). The OTR augmented by (13.22, 20.26, and 23.50 g/(m^2.day), respectively, similarly the OTR of the prepared CS/PVA/GE films is (8.45 g/(m2.day), which is less than the fabricated CS/PVA/GE/ZnO bionanocomposites films, which revealed OTR equal (10.78 g/(m^2.day)) the enhancement of the OTR of the prepared CS/PVA/GE/ZnO/Lg bionanocomposites due to the presence of ZnO nanoparticles and the lemon grass in the nanoform. The obtained results display the potential of CS/PVA/GE/ZnO/Lg bionanocomposites films for use as packaging materials for the modified atmosphere of the packaged materials.

Table 3. The permeability evaluation of the prepared CS/PVA/GE/ZnO/Lg bionanocomposites.

Samples	ZnO-NPs, %	Lg-NE, %	OTR, g/m^2.day	WVTR, g/m^2.day
CS/PVA/GE blend	0.0%	0.0%	8.45	2119.87
CS/PVA/GE/ZnO bionanocomposites	2%	0.0%	10.78	2013.56
CS/PVA/GE/ZnO/Lg bionanocomposites	2%	13.8%	13.22	1986.20
CS/PVA/GE/ZnO/Lg bionanocomposites	2%	20%	20.26	1848.31
CS/PVA/GE/ZnO/Lg bionanocomposites	2%	25%	23.50	1622.38

3.6. Mechanical studies of the prepared CS/PVA/GE/ZnO/Lg bionanocomposites.

The mechanical properties of the fabricated CS/PVA/GE blend, CS/PVA/GE/ZnO, and CS/PVA/GE/ZnO/Lg bionanocomposites containing different concentration of Lg-NE was described by tensile strength (TS) and elongation (E) tests. The characteristic tensile strengths are stated in (Table 4). An improvement in the mechanical performance of the prepared CS/PVA/GE/ZnO/Lg bionanocomposites associated with the CS/PVA/GE blend was detected. Furthermore, the addition of 2% of ZnO-NPs inside the CS/PVA/GE blend matrix improved the tensile strength (TS) from 3.3 MPa to 7.2 MPa, also the elongation increased from 22.6% to 26.9% in the case of using 2% ZnO-NPs inside CS/PVA/GE blend. When the different concentrations of Lg-NE in the presence of 2% ZnO-NPs content in the CS/PVA/GE/ZnO/Lg

bionanocomposites matrix, a significant rise of the TS was remarked, the additional loadings with 13.8, 20 and 25% of Lg-NE persuaded an improvement in tensile strength to 8.6, 9.3, and 10.4 MPa, respectively. Moreover, the elongation was enhanced by increasing the ratios of Lg-NE in the CS/PVA/GE/ZnO/Lg bionanocomposites to 28.7, 33.2, and 40.5, respectively, when using 13.8, 20, and 25% of Lg-NE into the bionanocomposites matrix. This tendency may be accredited to the interaction between ZnO-NPs and CS/PVA/GE blend and lemon grass nanoemulsion, which is a significant issue for enhancing the mechanical properties of the fabricated CS/PVA/GE/ZnO/Lg bionanocomposites.

Table 4. Mechanical properties of the prepared CS/PVA/GE/ZnO/Lg bionanocomposites.

Samples	ZnO-NPs, %	Lg-NE, %	Tensile strength, MPa	Elongation, %
CS/PVA/GE blend	0.0%	0.0%	3.3	22.6
CS/PVA/GE/ZnO bionanocomposites	2%	0.0%	7.2	26.9
CS/PVA/GE/ZnO/Lg bionanocomposites	2%	13.8%	8.6	28.7
CS/PVA/GE/ZnO/Lg bionanocomposites	2%	20%	9.3	33.2
CS/PVA/GE/ZnO/Lg bionanocomposites	2%	25%	10.4	40.5

3.7. Final contact angle of the prepared CS/PVA/GE/ZnO/Lg bionanocomposites.

The final contact angle was determined by a dynamic contact (OCA20) automated instrument angle via distilled water drop on the CS/PVA/GE blend and CS/PVA/GE/ZnO/Lg bionanocomposites containing different concentrations of LG-NE.

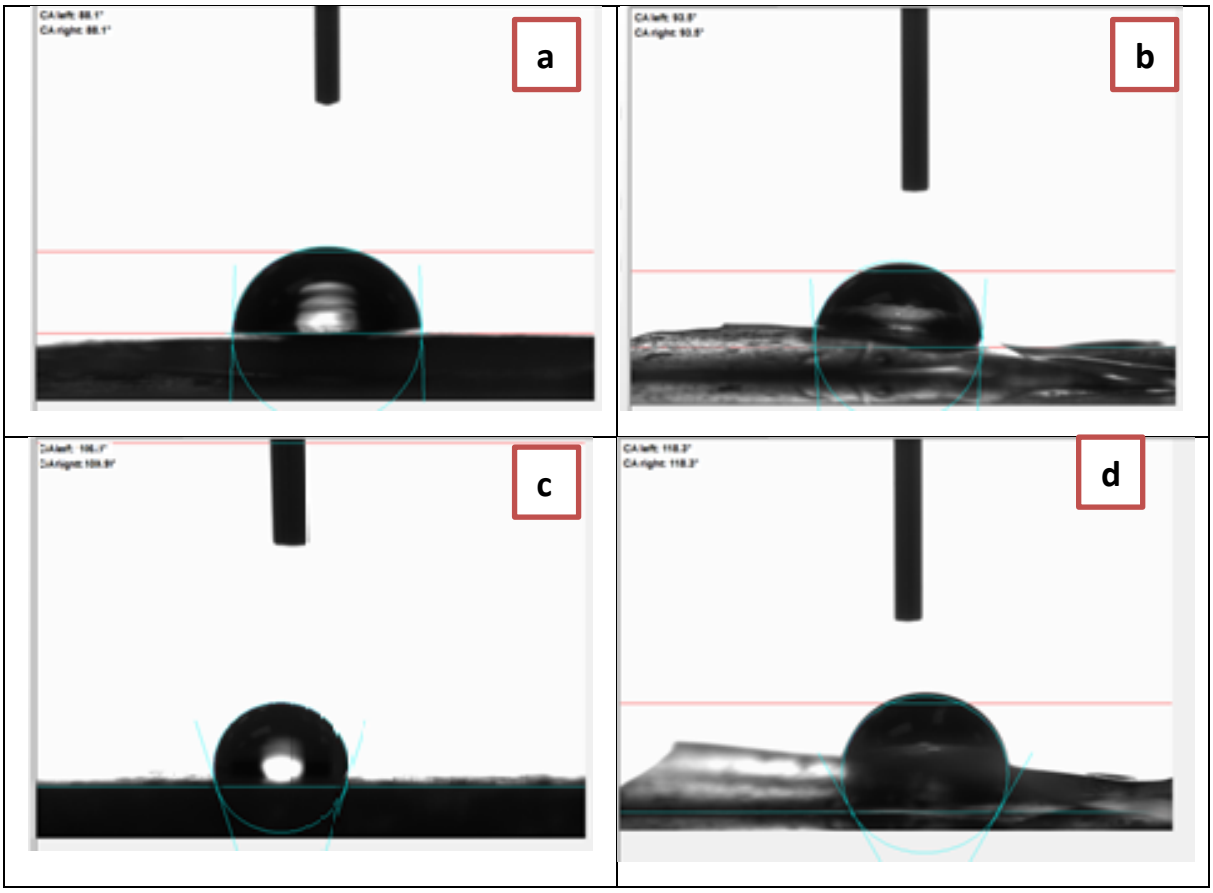

Figure 7. The final contact angle of **(a)** CS/PVA/GE blend; **(b)** CS/PVA/GE/ZnO as well as CS/PVA/GE/ZnO/Lg bionanocomposites containing different concentrations of Lg-NE; **(c)** 13.8 %; **(d)** 25%.

The final contact angles for CS/PVA/GE blend, as well as the CS/PVA/GE/ZnO/Lg bionanocomposites loaded with various ratios of Lg-NE and 2% ZnO-NPs, were presented in

(Figure 7). As declared in Figure 7, the final contact angle for CS/PVA/GE blend film was 88.1°, which exposed the occurrence of OH groups on the surface of CS/PVA/GE film. Similarly, the final contact angle values for CS/PVA/GE/ZnO bionanocomposites increased from 93.5° as ZnO-NPs content was 2%. Adding lemongrass in the nanoform to the CS/PVA/GE/ZnO bionanocomposites increased the final contact angles to 106.9 and 118.5 by increasing the ratios of Lg-NE from 13.8 to 25% in the presence of 2% ZnO-NPs in the bionanocomposite matrix. The achieved results indicate that increasing the concentration of Lg-NE confirmed an affinity to prevent the distribution of the water drop over the surface of CS/PVA/GE/ZnO/Lg bionanocomposites resulting in a rise of the surface hydrophobicity, as shown in (Figure 7).

3.8. Thermal properties evaluation of the prepared bionanocomposites.

The thermal stability of the prepared CS/PVA/GE/ZnO/Lg-NE bionanocomposites was assessed using a TGA instrument. Thermal stability was essential and deliberated as one of the main evaluations for materials used in food packaging applications since it is significant for packaging materials to control their processing temperature range and usage. Thus, the thermal stability of the prepared CS/PVA/GE blend and CS/PVA/GE/ZnO/Lg bionanocomposites were evaluated using thermal gravimetric analysis (TGA) from 25 to 600°C under air atmosphere, as revealed in Figure 8. All samples follow a similar decomposition trend. The CS/PVA/GE blend and CS/PVA/GE/ZnO/Lg bionanocomposites exhibited a three-step weight loss. The first minor weight loss (10%) step in the TGA curve below 100°C was attributed to the water evaporation of all samples. The second chief degradation step concerning rapid loss in weight between 150 and 470°C was assigned to the composite dehydration of the saccharide rings, depolymerization, and decay of the acetylated and deacetylated units of the polymers [45]. Moreover, the CS/PVA/GE/ZnO/Lg bionanocomposite displayed more thermal stability than CS/PVA/GE blend, and the char remains higher for the CS/PVA/GE/ZnO/Lg bionanocomposite that associated with the attendance of ZnO-NPs in the bionanocomposite matrix. Also, the thermal stability was increased by increasing the loadings of lemon grass nanoemulsion (Lg-NE) in the presence of constant ratios of ZnO-NPs, as revealed in (Figure 8). In contrast to these results, Nunes *et al*. [46] found that adding lemon nanoemulsion to gelatin film decreased the heat resistance due to lowering the gelatin matrix's intra/intermolecular protein interaction.

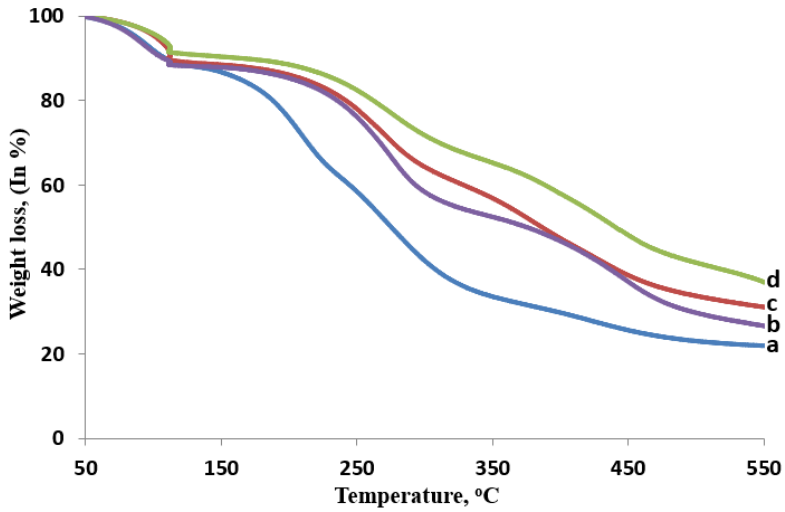

Figure 8. TGA curve of **(a)** CS/PVA/GE blend, as well as CS/PVA/GE/ZnO/Lg bionanocomposites containing different concentrations of Lg-NE; **(b)** 13.8 %; **(c)** 20%; **(d)** 25%.

3.9. Gel swelling property.

As shown in (Figure 9), it was clear that the highest swelling degree was found in T.H. "which did not contain neither Lg-NE nor ZnO-NPs" this may be owing to the hydrophilic characteristics of CH, PVA, and GE. However, T.A., which contains the highest Lg-NE" revealed the lowest swelling degree among all nanocomposite films being studied. It was obvious that all nanocomposite films incorporated with Lg-NE and ZnO-NPs had a lower swelling degree than those which did not contain Lg-NE or ZnO-NPs "T.H.". These results were in agreement with those reported in the contact angle and permeability tests.

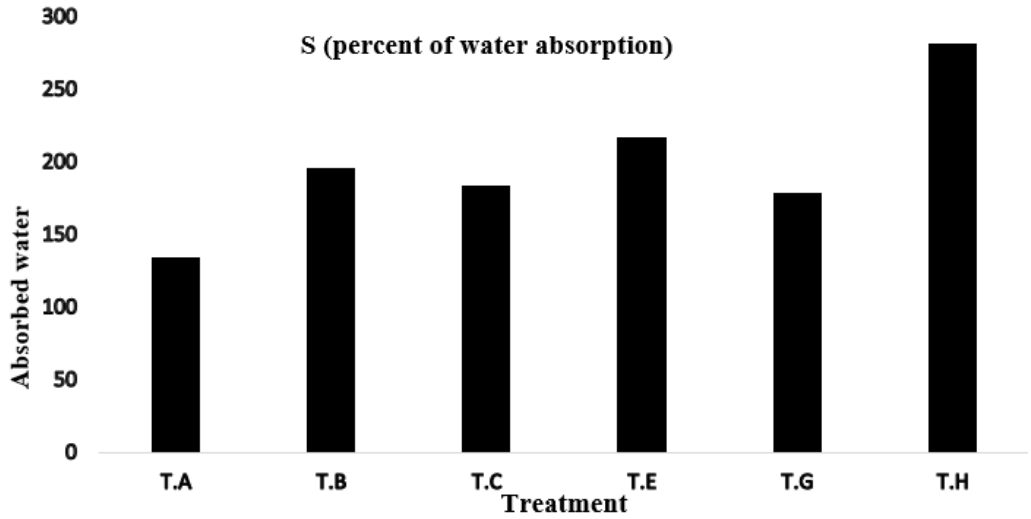

Figure 9. Gel swelling degree for CS/PVA/GE/ZnO/Lg bionanocomposite films.

3.9. Release of the Lemon grass essential oil from the nanocomposite film.

Figure 10 illustrates that the initial release of Lemon grass oil from CS/PVA/GE/ZnO/Lg bionanocomposites was started within 1st hour of the experiment and showed marked release in the oil till the 2nd day of storage, followed by slow and sustained release (up to 286 h) throughout times of experiment. Generally, the release of Lg-EO from the prepared nanocomposite into the food simulant is relatively slow.

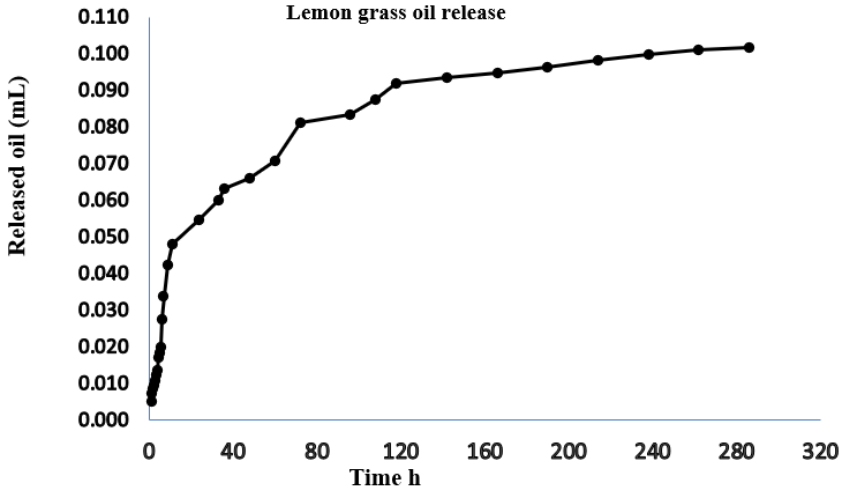

Figure 10. Oil Release Test for CS/PVA/GE/ZnO/Lg bionanocomposite film.

The causes of this phenomenon are due to the polarity of the film's component, the aldehyde group of the Lg-EO, and amino acid residues of the gelatin polymer chains can form

hydrogen bonds. Therefore, the antibacterial agent is not easy to be released from the films due to the large intermolecular force between CH, PVA, GE, and Lg-EO. The film showed less release rate due to properties such as high crystallization, high molecular weight, more structural density, and stronger connections with biopolymer chains, which is similar to the results reported by Aziz and Almasi [47].

3.10. Antimicrobial activity of Lemon grass essential oil and its nanoemulsion.

The obtained MIC and MLC of lemon grass essential oil and its nanoemulsion are presented in Table 5. For the tested Gram +ve bacteria, Listeria monocytogenes, MLC values of raw oil and its nanoemulsion were 2.5 and 0.625 µl /mL broth, while their MIC values were 1.25 and 0.31 µl /mL broth, respectively. For raw lemongrass oil, the obtained MIC was higher than that found by Barbosa *et al*., [48] $MIC_{90\%}$= 0.05% v/v; but lower than that found by T. L. C. de Oliveira *et al*., [49] "1.56%." As well, Cui *et al*. [50] reported higher values for MIC and MLC "0.5 mg/mL and 1.0 mg/mL, respectively". Regarding the tested Gram –ve bacteria, *Salmonella Typhimurium*, it was observed that lemon grass essential oil and its nanoemulsion had MLC values of 3.21 and 1.25 µl/mL broth and MIC values of 1.56 and 0.62 µl/mL broth, respectively. The previous result was proved to be less than that recorded by Hammer *et al*. [51], who found a MIC value of 0.25 (% v/v), and Tayel *et al*. [52], who found a MIC value of 550 micro g/mL.

Table 5. Minimum inhibitory concentration (MIC) and Minimum lethal concentration (MLC) of lemongrass oil (LGO) and its nanoemulsion (Lg-NE)

Antimicrobial agent	**MLC, (µl / mL)**		**MLC, (µl / mL)**	
	Salmonella Typhimurium	***Listeria Monocytogenes***	***Salmonella Typhimurium***	***Listeria Monocytogenes***
LGO	1.56	**1.25**	**3.21**	**2.50**
Lg-NE	0.62	**0.31**	**1.25**	**0.63**

It was noted that the oil's MIC and MLC values and nanoemulsion were higher for *Salmonella Typhimurium* (Gram – ve bacteria) than for Listeria monocytogenes (Gram +ve bacteria). These results were in agreement with Burt [53], and this may be due to the differences between the cell wall structures in both of them. Specifically, Gram-negative bacteria have more complex cell walls and outer membranes, so they act as barriers against antimicrobial compounds leading to higher resistance [54]. The MIC and MLC values of the nanoemulsion form were lowered than those reported for its raw form. This may be due to the reduced droplet size of the nanoemulsion showing enhanced antimicrobial efficacy due to their increased surface areas and its passive transport through the outer cell membrane [55–57].

3.11. Application of the prepared CS/PVA/GE/ZnO/Lg-NE bionanocomposites on chilled chicken meat samples for evaluating their physicochemical and microbiological effects.

3.11.1. Physicochemical evaluation of chicken meat samples.

3.11.1.1. Sensory evaluation.

The data presented in (Fig. 11) clarify the changes that happened to the sensory profile of packaged chilled chicken meat samples throughout the storage period. It was clear that at 0

times, all treatments were bright pink in color, shiny, wet, and not sticky, recovered immediately, and had a fresh smell (score 5). After 24 h, the score decreased to score 3 (red, dull, non-wet but sticky, recovered slowly and a little off-flavor) for the control sample to a score 4 (pink, a little shiny, little wet but not sticky, recovered slowly, no abnormal odor) for treatments T. C, T. D, T.F, T. G, and T. H, while samples of treatments T.A, T.B, and T.E kept sensory score of 5. On the third day, the control sample became sensorial unacceptable (score 1). Samples of treatments T.G and T.H got scores of 3, while the other treatments all displayed scores of 4. on day 5 of storage, only treatments T.A, T.B, and T.E kept score 4, whilst other treatments became unacceptable (score 2). As well, T. A and T. B were rejected on the 7th day of storage (the end of the experiment).

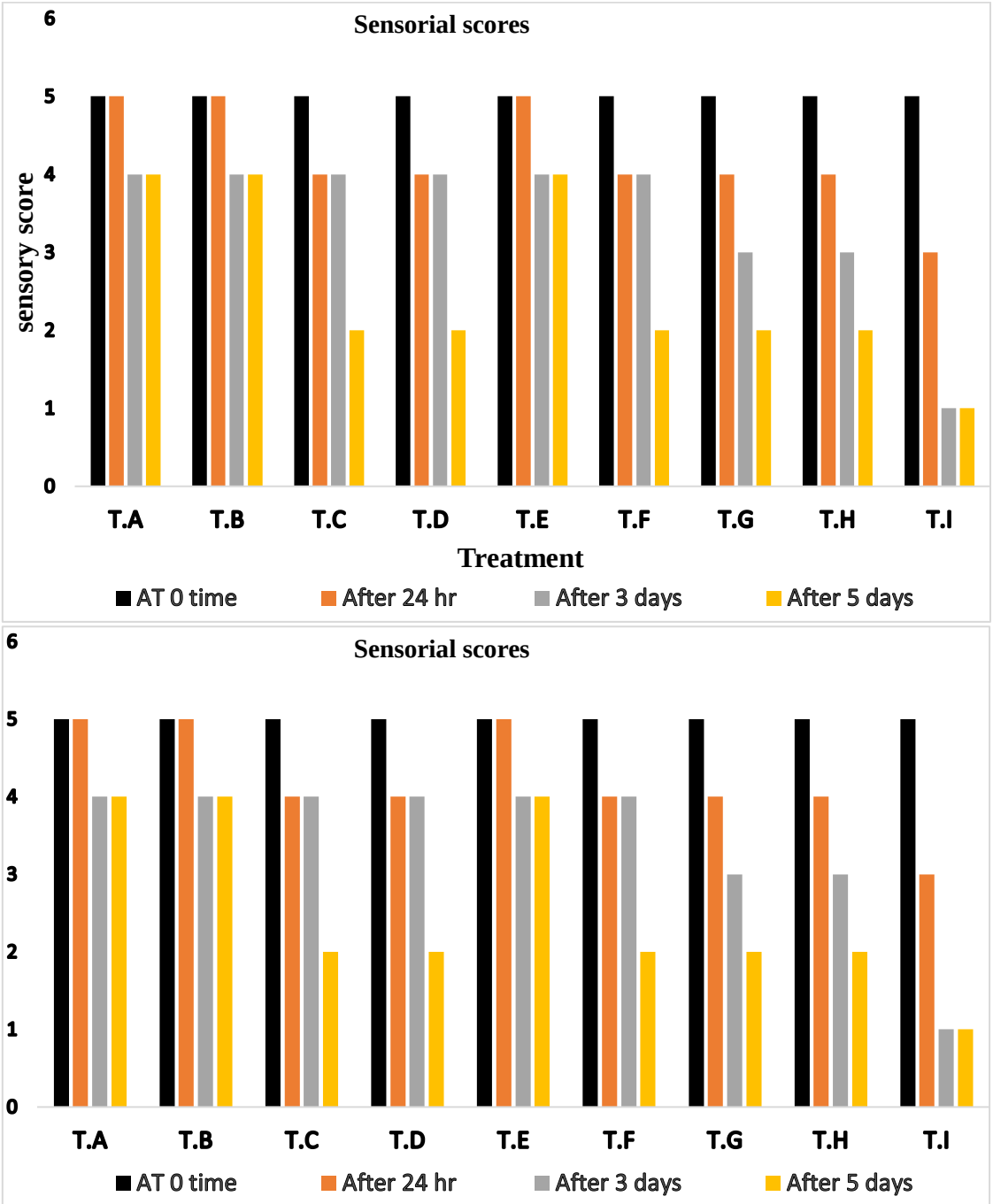

Figure 11. Sensory evaluation of chicken meat wrapped by the prepared CS/PVA/GE/ZnO/Lg bionanocomposites.

Overall, T.A and T.B, which have the highest ratios of Lg-NE, showed the best influence on the sensory characteristics of the packaged chilled chicken meat samples. Using the oil in the nano form showed no impact on the odor of the packed sample either in its raw state or after cooking and enhanced the general physical condition. Moreover, the results stated by Kim *et al*. [58]. Ahmad *et al*. [59] and Tayel *et al*. [52] were in agreement with the current results. However, T. L. C. de Oliveira *et al*. [49] declared that directly adding lemon grass essential oil into bovine ground meat at concentrations higher than 1.56% produces undesirable changes in taste, odor, and characteristic color. In addition, Kamona and Alzobaay [60] found that lemongrass essential oil improved the sensorial properties, color, texture, flavor, taste, and overall acceptability of fish meatballs.

3.11.1.2. Determination of pH.

Figure 12a illustrates that the initial pH value of the fresh samples (controls and treatments) was 6.32 (time zero). Twenty-four hours later, the pH decreased to in the range of 5.81 to 6.69. After 3 days, samples of treatments T.B, T.C, and T. E showed the lowest pH values of 6.01, 5.8, and 5.89, respectively. On the fifth day, the pH of T.A, T.B, and T.E were 6.07, 6.2, and 6.05, respectively, while samples of other treatments were sensory unaccepted. At the end of the storage period T.A, T.B, and T. E showed values lower than those reported at 0 times. Generally, wrapping samples with CS/PVA/GE/ZnO/Lg bionanocomposites enhanced their pH values throughout the storage period. Similar findings were proved by Ahmad *et al*. [59] and Kieling *et al*. [61].

3.11.1.3. Determination of Thiobarbituric Acid Reactive Substances (TBARS).

The results of thiobarbituric acid reactive substances (TBARS) of chilled poultry meat samples wrapped with or without nanocomposite films are presented in Figure 12 b. It was obvious that the TBARS value of samples showed an oscillation over storage time but did not exceed the permissible limit (0.9 mg malonaldehyde/kg sample). Lower values of TBARS were recorded in samples of T.B and T.E at the end of the storage period (fifth day) than their initial values, which indicated that lemongrass nanoemulsion had an antioxidant effect reducing the thiobarbituric acid reactive substance value. The reduction in TBARS value could be explained by the low oxygen permeability characteristics of nanocomposite films incorporated with LG NE besides its antioxidant activity [62]. As well, lemon grass essential oil act as an effective free radical scavenger and metal chelating agent, interrupting the lipid oxidation chain reaction [63].

Similar outcomes were obtained by Olorunsanya *et al*. [64], Ahmad *et al*. [59], and Kieling *et al*. [61], who proved that lemongrass essential oil had a reduction effect on TBARS value. Samples wrapped with CH/PVA/GE/ZnO-NPS film (T. G) and CH/PVA/GE film (T. H), regardless of LEO incorporated, showed a reduction in TBARS values superior to that recorded in the control sample proved that the film components have an antioxidant effect, which agreed with the results of Ahmad *et al*., [59] and Singh *et al*., [65]. Overall, it could be concluded that lemongrass essential oil has an antioxidant effect that is consistent with the findings of numerous studies [66–70].

3.11.2. Microbiological examination of chicken meat samples wrapped with the prepared bionanocomposite films.

3.11.2.1. Total yeast count.

As presented in Figure 12 c, the initial total yeast count of all tested samples and control was 3.334 log CFU/g. After 24 h, a marked reduction occurred in yeast count in all treatments except in T.D, which showed an increase in the count by one log and control increased by 2 logs. The reduction rate in treatments of T. A, T. B, T. C, T. E, and T. F were 33.5, 8.99, 19.79, 8.99, and 73.78%, respectively. At the same time, the T. G and T. H revealed no changes in the count. Following that, on the third day of storage, the count increased in samples of T. B, T. C, T. D, and T. H treatments by approximately 1:2 log CFU/g while it remained constant in samples of T. F and T.G and continuously decreased in samples of T.A and T.E. Finally, treatment A showed a continuous decline. However, T. B and T. E revealed a prominent increase in the count on the fifth day of storage. Simultaneously, the other treatments were rejected organoleptically and were removed from the trial.

Generally, some treatments; that had the highest lemongrass percentage; showed a sustained decline in the yeast count throughout the entire trial (T. A and T.F). In contrast, T. D and T. I showed a continual increase in the count throughout the experiment. However, other treatments showed some oscillation in their count throughout the trial (T. B, T. C, and T. E). Additionally, T. G showed the same count throughout the entire trial period.

In conclusion, the previous outcome indicated that the perfect treatment for the reduction of total yeast count throughout the storage time was T. A. It is indicated that the nanocomposite film's efficiency improved by increasing the concentration of lemon grass nanoemulsion incorporated within the prepared film. These results were in agreement with those of Sacchetti *et al*. [71] and Naik *et al*. [72].

3.11.2.2. Total mold count.

As illustrated in Figure 12 d, the initial total mold count was 3.49 log cfu/g for all treatments.

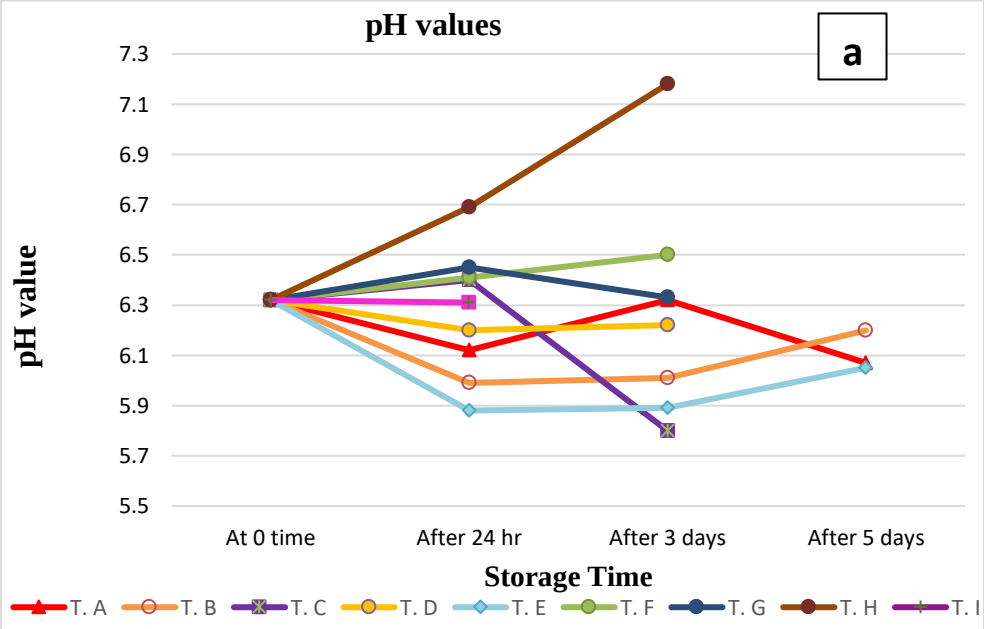

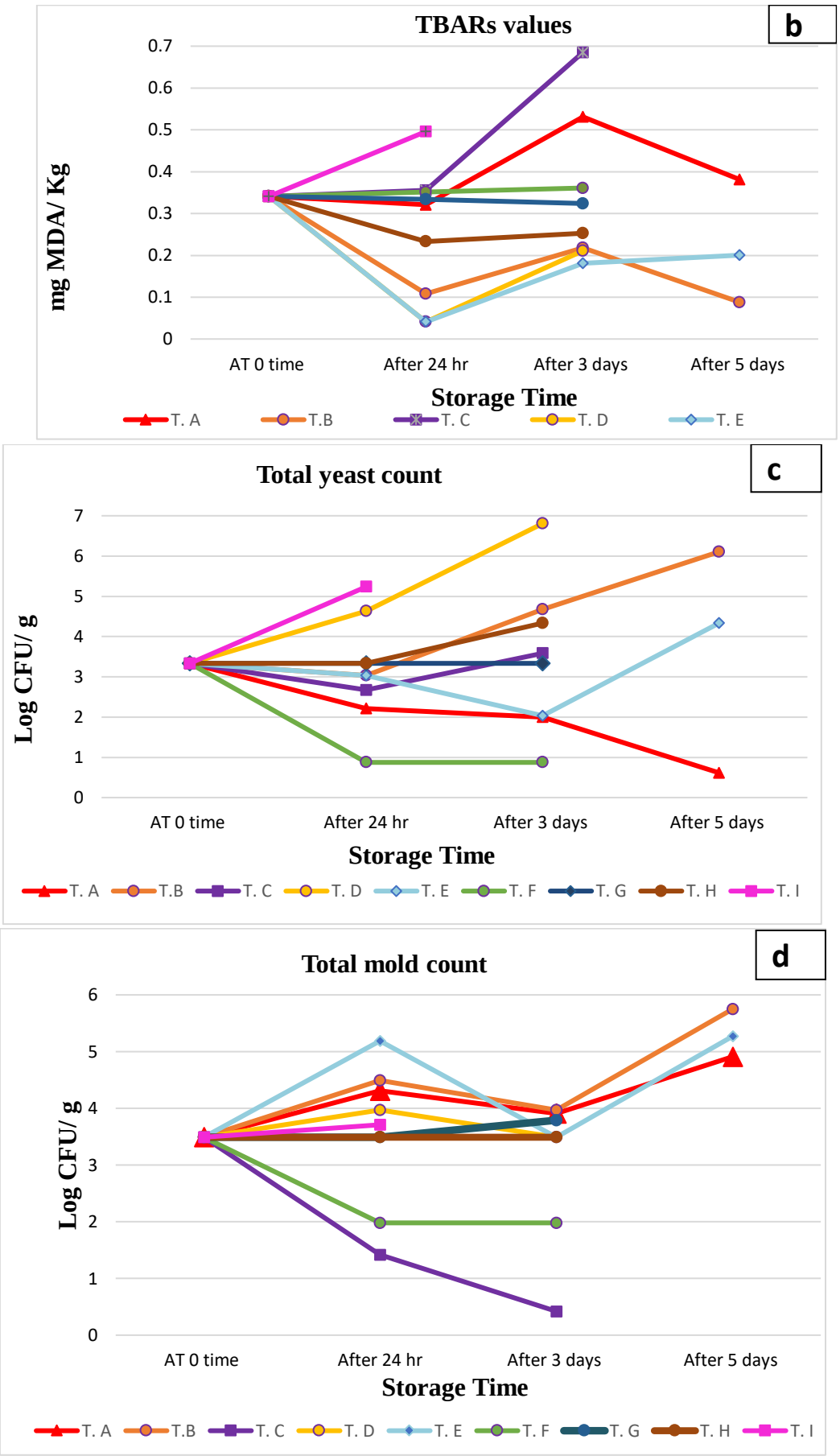

Figure 12. Chemical and Microbiological examination of chicken meat samples wrapped by the prepared bionanocomposite films.

After 24 h, most treatments showed a rise in the total mold count except T. C and T. F, which revealed a prominent decline in the count with a reduction rate of 59.3 and 43.26%, respectively. In contrast, T. G and T.H showed no change in the count. Examination of the samples on the third day of storage revealed that five treatments (T.A, T.B, T.C, T.D, and T.E) out of nine had a decline in the count, whilst T. F and T.H showed no change in counts to those documented at the previous examination. Furthermore, T. G had a slight increase in the count on the third day. However, control became unaccepted organoleptically and was removed from the trial. On the fifth day, an increase in the count was declared in treatments T.A, T. B, and T. E, whereas other treatments were unaccepted organoleptically and discarded.

Generally, it was noticed that treatments T. C and T.F showed a continuous decline in the count until their sensory spoilage with a reduced rate on their third day of 87.96 and 43.26%, respectively. Treatment T. H revealed a constant count throughout the experiment, whereas T. G revealed a constant value during the first two examinations, then showed a slight increase on the third day. It was noticed that the blank films, despite containing neither lemongrass nanoemulsion nor ZnO-NPs, prevented mold growth and ceased their multiplication. The obtained results indicated that Lg-NE incorporation within the prepared nanocomposite films enhanced their antifungal effect. Furthermore, many studies agree with the previous results [73–76]. Cofelice *et al*. [77] mentioned that Lemongrass nanoemulsion had an inhibitory effect on Rhizopus spp., *Penicillium expansum* and *Aspergillus niger*.

3.12. Challenge study.

3.12.1. Effect of the prepared bionanocomposites on *Salmonella Typhimurium* count:

Variations in the value of salmonella count during refrigerated storage are presented in (Figure 13a) the initial count in the control sample and treatments was 6.18 log cfu/g. After 24 h, all treatments had a prominent decline in the count except for T. A and T. G, which showed an increase in their count. The reduction rates were 43.36, 18.9, 24.75, 27.99, and 9.38% for treatments T.B, T.C, T.E, T.H, and T.I, respectively. Nevertheless, on the third day of storage, all treatments, T. A, T. B, T.C, T.E, T.G, and T. H, showed a marked decrease in the count, with a reduced rate of 40.12, 49.93, 34.14, 45.79, 31.06, and 39.32%, respectively. It was also observed that all treatments on the fifth day of storage had counts lower than those observed at zero time with reduction rates of 30.42, 33.65, 9.54, 49.83, 29.61, and 30.9%, respectively, and 15.85% for the control sample. A reduction in the count was observed in the control samples. However, the reduction rate was lower than that reported for the treatments, especially for T.A, T.B, and T. E. After 7 days of storage also, all treatments had counts lower than their initial count with variation in the reduction rate, which ranged from a minimum value of 14.88% for T. A to a maximum value of 59.54% for T. E. Simultaneously, the control treatment became unacceptable organoleptically and was rejected. Ten days after the beginning of the trial, most treatments (T.C, T.E, T.G, and T.H) had counts higher than those at the previous examination. However, the count was lower than that reported at zero time, with reduced rates of 35.76, 44.98, 33.65, and 42.23, respectively. T.A. revealed that the Salmonella count on the tenth day of storage was lower than the previous examination, with a reduced rate of 35.27% from its count at zero time.

At the end of the storage period, it was obvious that most treatments (T.A, T.C, and T.E) increased in the count than the previous examination but were still lower than the initial count with reduction rates of 23.95, 28.64, and 30.58%, respectively. It was observed that the

reduction rate increased with the increase in the oil nanoemulsion concentration. Consistent with the previous result, Tayel *et al*. [52]; Kim *et al*. [58], and Oh *et al*. [78] documented that lemon grass nanoemulsion or extract has an inhibitory effect on *Salmonella Typhimurium*. Additionally, Dewi *et al*. [79] mentioned that lemongrass essential oil was effective against Salmonella Heidelbeg *in vitro* and on the pathogen's attachment to poultry skin and meat. As well, gelatin nanofibers with lemongrass essential oil (Gt/LEO) showed a 96.63% inhibition rate against *Salmonella Typhimurium* [80].

3.12.2. Effect of the prepared bionanocomposites on *Listeria monocytogenes count*.

The data presented in (Figure 13b) describe the changes in Listeria monocytogenes count in chicken meat samples wrapped with the prepared nanocomposite films throughout the storage period at 4°C.

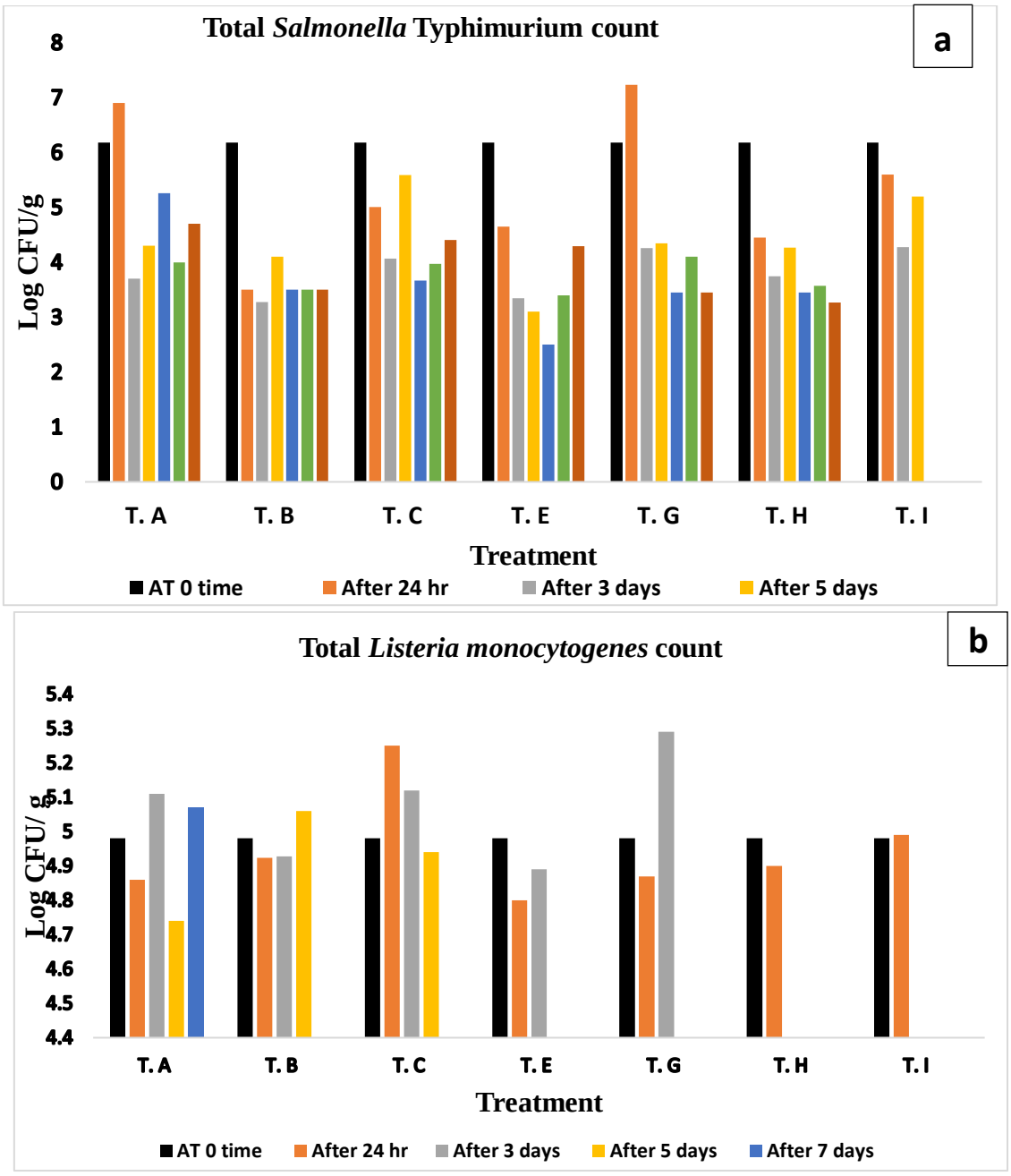

Figure 13. Total *Salmonella Typhimurium and Listeria monocytogenes* count of chicken meat samples wrapped by the prepared CS/PVA/GE/ZnO/Lg bionanocomposites.

The initial count (zero time) was 4.98 log cfu/g for the control and other treatments. All treatments showed a weak reduction rate throughout their storage period, which extended to 10 days for T.A; 7 days for T.B and T.C; 5 days for T.E and T.G. However, T.H. and T.I were rejected organoleptically on the third day of storage and showed no reduction in the count, whereas T.A showed the highest reduction rate (4.8%) on the fifth day of storage. Our findings were in partial compliance with the previous studies, as the higher concentration of the nanoemulsion showed a slight inhibitory effect on the growth of Listeria monocytogenes. At the end of the storage, T. A exhibited a higher count than that on the fifth day and at zero time. The previous findings proved that lemongrass essential oil has bactericidal activity against *L. monocytogenes* [50,68,81–85].

4. Conclusions

In the current work, the lemon grass nanoemulsion (Lg-NE) and Zinc oxide nanoparticles (ZnO-NPs) were prepared and characterized by dynamic light scattering (DLS) and TEM analysis to confirm their nanoform with particle size around 335 nm for ZnO-NPs and 378 nm for Lg-NE by DLS. Furthermore, nanocomposite films CS/PVA/GE/ZnO/Lg were prepared with different ratios of Lg-NE by solution and casting technique. The prepared films were characterized using XRD, FTIR, and SEM, which indicate interactions between various components of the biodegradable film. In addition, the thermal, mechanical, and permeability characteristics of CS/PVA/GE/ZnO/Lg-NE bionanocomposite and blank films were assessed. It can be concluded that by raising the concentration of Lg-NE in the bionanocomposite matrix, the compatibility between the three-biopolymer and the Lg-NE incorporated into the polymer chains in the presence of ZnO-NPs, increased, which leads to improving oxygen permeability from 8.45 to 23.50 g/m^2.day, the Tensile strength was improved from 3.3 MPa for CS/PVA blend to 10.4 MPa for CS/PVA/GE/ZnO/Lg-NE containing 25 % of Lg-NE and thermal properties of the prepared CS/PVA/GE/ZnO/Lg-NE bionanocomposite was enhanced by the addition of Lg-NE from13.8 %, d) 25%. The prepared CS/PVA/GE/ZnO/Lg-NE films enhanced the sensory characteristics of the chilled chicken meat parts, as well it revealed antioxidant, antibacterial, and antifungal influences on the wrapped samples. As well as, films have lowered the population of the tested pathogenic food microorganisms, *Listeria monocytogenes*, and *Salmonella Typhimurium*, throughout the storage period. Moreover, it was proved that there is a synergistic effect between Lg-NE and ZnO-NPs, enhancing the film's characteristics and antimicrobial effect on chilled chicken meat parts.

Funding

This research received no external funding.

Acknowledgments

The authors wish to gratefully acknowledge National Research Centre (NRC), Egypt, for supporting the current work.

Conflicts of Interest

The authors declare no conflict of interest.

References

1. Al-Hijazeen, M.; Lee, E.J.; Mendonca, A.; Ahn, D.U. Effect of Oregano Essential Oil (Origanum Vulgare Subsp. Hirtum) on the Storage Stability and Quality Parameters of Ground Chicken Breast Meat. *Antioxidants* **2016**, *5*, 18, https://doi.org/10.3390/antiox5020018.
2. Takma, D.K.; Korel, F. Active Packaging Films as a Carrier of Black Cumin Essential Oil: Development and Effect on Quality and Shelf-Life of Chicken Breast Meat. *Food Packag. Shelf Life* **2019**, *19*, 210–217, https://doi.org/10.1016/j.fpsl.2018.11.002.
3. Díaz-Montes, E.; Castro-Muñoz, R. Edible Films and Coatings as Food-Quality Preservers: An Overview. *Foods* **2021**, 10, 249 2021, https://dx.doi.org/10.3390/foods10020249.
4. Primožič, M.; Knez, Ž.; Leitgeb, M. (Bio)Nanotechnology in Food Science—Food Packaging. *Nanomaterials* **2021**, *11*, 292, https://doi.org/10.3390/nano11020292.
5. Sánchez-Ortega, I.; García-Almendárez, B.E.; Santos-López, E.M.; Amaro-Reyes, A.; Barboza-Corona, J.E.; Regalado, C. Antimicrobial Edible Films and Coatings for Meat and Meat Products Preservation. *Sci. World J.* **2014**, *2014*, https://doi.org/10.1155/2014/248935.
6. Rathod, N.B.; Bangar, S.P.; Šimat, V.; Ozogul, F. Chitosan and Gelatine Biopolymer-based Active/Biodegradable Packaging for the Preservation of Fish and Fishery Products. *Int. J. Food Sci. Technol.* **2022**, https://doi.org/10.1111/ijfs.16038.
7. Youssef, A. M.; El-Sayed, H. S.; Islam, E. N.; & El-Sayed, S. M. Preparation and characterization of novel bionanocomposites based on garlic extract for preserving fresh Nile tilapia fish fillets. *RSC adv*, 2021, *11*(37), 22571-22584. DOI: 10.1039/D1RA03819B
8. Said, N.S.; Sarbon, N.M. Physical and Mechanical Characteristics of Gelatin-Based Films as a Potential Food Packaging Material: A Review. *Membranes (Basel).* **2022**, *12*, 442, https://doi.org/10.3390/membranes12050442.
9. Hasanin, M. S., & Youssef, A. M. Ecofriendly bioactive film doped CuO nanoparticles based biopolymers and reinforced by enzymatically modified nanocellulose fibers for active packaging applications. *Food Packaging and Shelf Life*, 2022, *34*, 100979. https://doi.org/10.1016/j.fpsl.2022.100979
10. Ghaderi, J.; Hosseini, S.F.; Keyvani, N.; Gómez-Guillén, M.C. Polymer Blending Effects on the Physicochemical and Structural Features of the Chitosan/Poly (Vinyl Alcohol)/Fish Gelatin Ternary Biodegradable Films. *Food Hydrocoll.* **2019**, *95*, 122–132, https://doi.org/10.1016/j.foodhyd.2019.04.021.
11. Souza, V.G.L.; Rodrigues, C.; Valente, S.; Pimenta, C.; Pires, J.R.A.; Alves, M.M.; Santos, C.F.; Coelhoso, I.M.; Fernando, A.L. Eco-Friendly ZnO/Chitosan Bionanocomposites Films for Packaging of Fresh Poultry Meat. *Coatings* **2020**, *10*, 110, https://doi.org/10.3390/coatings10020110.
12. Moustafa, H.; El-Sayed, S. M.; & Youssef, A. M. Synergistic impact of cumin essential oil on enhancing of UV-blocking and antibacterial activity of biodegradable poly (butylene adipate-co-terephthalate)/clay platelets nanocomposites. *Journal of Thermoplastic Composite Materials*, 2013, *36*(1), 96-117. DOI: 10.1177/0892705721989771
13. Teixeira, B.; Marques, A.; Pires, C.; Ramos, C.; Batista, I.; Saraiva, J.A.; Nunes, M.L. Characterization of Fish Protein Films Incorporated with Essential Oils of Clove, Garlic and Origanum: Physical, Antioxidant and Antibacterial Properties. *LWT-Food Sci. Technol.* **2014**, *59*, 533–539, https://doi.org/10.1016/j.lwt.2014.04.024.
14. Cofelice, M.; Cuomo, F.; Chiralt, A. Alginate Films Encapsulating Lemongrass Essential Oil as Affected by Spray Calcium Application. *Colloids and Interfaces* **2019**, *3*, 58, https://doi.org/10.3390/colloids3030058.
15. Cheel, J.; Theoduloz, C.; Rodríguez, J.; Schmeda-Hirschmann, G. Free Radical Scavengers and Antioxidants from Lemongrass (Cymbopogon Citratus (DC.) Stapf.). *J. Agric. Food Chem.* **2005**, *53*, 2511–2517, https://doi.org/10.1021/jf0479766.
16. Fisher, K.; Phillips, C.A. The Effect of Lemon, Orange and Bergamot Essential Oils and Their Components on the Survival of Campylobacter Jejuni, Escherichia Coli O157, Listeria Monocytogenes, Bacillus Cereus and Staphylococcus Aureus *in vitro* and in Food Systems. *J. Appl. Microbiol.* **2006**, *101*, 1232–1240, https://doi.org/10.1111/j.1365-2672.2006.03035.x.
17. Kamaruddin, Z.H.; Jumaidin, R.; Selamat, M.Z.; Ilyas, R.A. Characteristics and Properties of Lemongrass (Cymbopogan Citratus): A Comprehensive Review. *J. Nat. Fibers* **2021**, *19*, 1–18, https://doi.org/10.1080/15440478.2021.1958439.
18. Faheem, F.; Liu, Z.W.; Rabail, R.; Haq, I.-U.; Gul, M.; Bryła, M.; Roszko, M.; Kieliszek, M.; Din, A.; Aadil, R.M. Uncovering the Industrial Potentials of Lemongrass Essential Oil as a Food Preservative: A Review.

Antioxidants **2022**, *11*, 720, https://doi.org/10.3390/antiox11040720.
19. Sánchez-González, L.; Chiralt, A.; González-Martínez, C.; Cháfer, M. Effect of Essential Oils on Properties of Film Forming Emulsions and Films Based on Hydroxypropylmethylcellulose and Chitosan. *J. Food Eng.* **2011**, *105*, 246–253, https://doi.org/10.1016/j.jfoodeng.2011.02.028.
20. Kong, I.; Degraeve, P.; Pui, L.P. Polysaccharide-Based Edible Films Incorporated with Essential Oil Nanoemulsions: Physico-Chemical, Mechanical Properties and Its Application in Food Preservation—A Review. *Foods* **2022**, *11*, 555, https://doi.org/10.3390/foods11040555.
21. B, D.; Girigoswami, A.; Girigoswami, K. Antimicrobial, Pesticidal and Food Preservative Applications of Lemongrass Oil Nanoemulsion: A Mini-Review. *Recent Pat. Food. Nutr. Agric.* **2022**, *12*, https://doi.org/10.2174/2212798412666220527154707.
22. Aewsiri, T.; Benjakul, S.; Visessanguan, W.; Wierenga, P.A.; Gruppen, H. Antioxidative Activity and Emulsifying Properties of Cuttlefish Skin Gelatin–Tannic Acid Complex as Influenced by Types of Interaction. *Innov. food Sci. Emerg. Technol.* **2010**, *11*, 712–720, https://doi.org/10.1016/j.ifset.2010.04.001.
23. Cota-Arriola, O.; Onofre Cortez-Rocha, M.; Burgos-Hernández, A.; Marina Ezquerra-Brauer, J.; Plascencia-Jatomea, M. Controlled Release Matrices and Micro/Nanoparticles of Chitosan with Antimicrobial Potential: Development of New Strategies for Microbial Control in Agriculture. *J. Sci. Food Agric.* **2013**, *93*, 1525–1536, https://doi.org/10.1002/jsfa.6060.
24. Youssef, A. M.; El-Sayed, H. S.; El-Sayed, S. M.; Fouly, M.; & Abd El-Aziz, M. E. Novel bionanocomposites based on cinnamon nanoemulsion and TiO2-NPs for preserving fresh chicken breast fillets. Food Bioprocess Technol. 2023, 16, 356–367 (2023). https://doi.org/10.1007/s11947-022-02934-w
25. Kumar, S.; Boro, J.C.; Ray, D.; Mukherjee, A.; Dutta, J. Bionanocomposite Films of Agar Incorporated with ZnO Nanoparticles as an Active Packaging Material for Shelf Life Extension of Green Grape. *Heliyon* **2019**, *5*, e01867, https://doi.org/10.1016/j.heliyon.2019.e01867.
26. Youssef, A.M.; Assem, F.M.; Abdel-Aziz, M.E.; Elaaser, M.; Ibrahim, O.A.; Mahmoud, M.; Abd El-Salam, M.H. Development of Bionanocomposite Materials and Its Use in Coating of Ras Cheese. *Food Chem.* **2019**, *270*, 467–475, https://doi.org/10.1016/j.foodchem.2018.07.114.
27. Giske, C.G.; Turnidge, J.; Cantón, R.; Kahlmeter, G. Update from the European Committee on Antimicrobial Susceptibility Testing (EUCAST). *J. Clin. Microbiol.* **2022**, *60*, e00276-21, https://doi.org/10.1128/jcm.00276-21.
28. Ghosh, V.; Mukherjee, A.; Chandrasekaran, N. Ultrasonic Emulsification of Food-Grade Nanoemulsion Formulation and Evaluation of Its Bactericidal Activity. *Ultrason. Sonochem.* **2013**, *20*, 338–344, https://doi.org/10.1016/j.ultsonch.2012.08.010.
29. Standards, N.C. for C.L. Methods for Dilution Antimicrobial Susceptibility Tests for Bacteria That Grow Aerobically—Tenth Edition:(Approved Standard M7-A10) **2015**.
30. EFSA Panel on Food Contact Materials, E. and P.A. (CEP); Silano, V.; Barat Baviera, J.M.; Bolognesi, C.; Chesson, A.; Cocconcelli, P.S.; Crebelli, R.; Gott, D.M.; Grob, K.; Lambré, C. Review and Priority Setting for Substances That Are Listed without a Specific Migration Limit in Table 1 of Annex 1 of Regulation 10/2011 on Plastic Materials and Articles Intended to Come into Contact with Food. *EFSA J.* **2020**, *18*, e06124, https://doi.org/10.2903/j.efsa.2020.6124.
31. Bustos C, R.O.; Alberti R, F. V; Matiacevich, S.B. Edible Antimicrobial Films Based on Microencapsulated Lemongrass Oil. *J. Food Sci. Technol.* **2016**, *53*, 832–839, https://doi.org/10.1007/s13197-015-2027-5.
32. El-Sayed, S. M.; El-Sayed, H. S.; Elgamily, H. M.; & Youssef, A. M. Preparation and evaluation of yogurt fortified with probiotics jelly candy enriched with grape seeds extract nanoemulsion. Journal of Food Processing and Preservation, 2022, 46(7), e16713. https://doi.org/10.1111/jfpp.16713
33. Lu, W.; Wu, Y.; Guo, Q.; Ren, L.; Zhu, P.; Xu, L.; Chang, G.; Chen, G. Establishment of a Freshness-Evaluating Standard for Chilled Yellow Chicken Meat. *Food Anal. Methods* **2017**, *10*, 2629–2635, https://doi.org/10.1007/s12161-017-0815-4%0A%0A.
34. Buege, J.A.; Aust, S.D. Microsomal Lipid Peroxidation. Me-Thods Enzymol. **1978**, *52*, 302-310. https://dx.doi.org/10.1016/S0076-6879(78)52032-6.
35. Hungerford, L.L.; Campbell, C.L.; Smith, A.R. *Veterinary Mycology Laboratory Manual.*; Iowa State University Press, 1998; ISBN 081382849X, https://agris.fao.org/agris-search/search.do?recordID=US201300024303.
36. Morsy, M.K.; Khalaf, H.H.; Sharoba, A.M.; El-Tanahi, H.H.; Cutter, C.N. Incorporation of Essential Oils and Nanoparticles in Pullulan Films to Control Foodborne Pathogens on Meat and Poultry Products. *J. Food Sci.* **2014**, *79*, M675–M684, https://doi.org/10.1111/1750-3841.12400.

37. Cutter, C.N.; Siragusa, G.R. Efficacy of Organic Acids Against Escherichia Coli O157: H7 Attached to Beef Carcass Tissue Using a Pilot Scale Model Carcass Washer1. *J. Food Prot.* **1994**, *57*, 97–103, https://doi.org/10.4315/0362-028X-57.2.97.
38. Nguyen, V.T.; Gidley, M.J.; Dykes, G.A. Potential of a Nisin-Containing Bacterial Cellulose Film to Inhibit Listeria Monocytogenes on Processed Meats. *Food Microbiol.* **2008**, *25*, 471–478, https://doi.org/10.1016/j.fm.2008.01.004.
39. Trinetta, V.; Floros, J.D.; Cutter, C.N. Sakacin A-containing Pullulan Film: An Active Packaging System to Control Epidemic Clones of Listeria Monocytogenes in Ready-to-eat Foods. *J. Food Saf.* **2010**, *30*, 366–381, https://doi.org/10.1111/j.1745-4565.2010.00213.x.
40. Kumar, S.; Mudai, A.; Roy, B.; Basumatary, I.B.; Mukherjee, A.; Dutta, J. Biodegradable Hybrid Nanocomposite of Chitosan/Gelatin and Green Synthesized Zinc Oxide Nanoparticles for Food Packaging. *Foods* **2020**, *9*, 1143, https://doi.org/10.3390/foods9091143.
41. Soltanzadeh, M.; Peighambardoust, S.H.; Ghanbarzadeh, B.; Mohammadi, M.; Lorenzo, J.M. Chitosan Nanoparticles Encapsulating Lemongrass (Cymbopogon Commutatus) Essential Oil: Physicochemical, Structural, Antimicrobial and in-Vitro Release Properties. *Int. J. Biol. Macromol.* **2021**, *192*, 1084–1097, https://doi.org/10.1016/j.ijbiomac.2021.10.070.
42. Wang, T.; Turhan, M.; Gunasekaran, S. Selected Properties of PH-sensitive, Biodegradable Chitosan–Poly (Vinyl Alcohol) Hydrogel. *Polym. Int.* **2004**, *53*, 911–918, https://doi.org/10.1002/pi.1461.
43. Brugnerotto, J.; Lizardi, J.; Goycoolea, F.M.; Argüelles-Monal, W.; Desbrieres, J.; Rinaudo, M. An Infrared Investigation in Relation with Chitin and Chitosan Characterization. *Polymer (Guildf).* **2001**, *42*, 3569–3580, https://doi.org/10.1016/S0032-3861(00)00713-8.
44. Mansur, H.S.; Costa, H.S. Nanostructured Poly (Vinyl Alcohol)/Bioactive Glass and Poly (Vinyl Alcohol)/Chitosan/Bioactive Glass Hybrid Scaffolds for Biomedical Applications. *Chem. Eng. J.* **2008**, *137*, 72–83, https://doi.org/10.1016/j.cej.2007.09.036.
45. Youssef, A.M.; El-Sayed, S.M.; Salama, H.H.; El-Sayed, H.S.; Dufresne, A. Evaluation of Bionanocomposites as Packaging Material on Properties of Soft White Cheese during Storage Period. *Carbohydr. Polym.* **2015**, *132*, 274–285, https://doi.org/10.1016/j.carbpol.2015.06.075.
46. Nunes, J.C.; Melo, P.T.S.; Lorevice, M.V.; Aouada, F.A.; de Moura, M.R. Effect of Green Tea Extract on Gelatin-Based Films Incorporated with Lemon Essential Oil. *J. Food Sci. Technol.* **2021**, *58*, 1–8, https://doi.org/10.1007/s13197-020-04469-4%0A%0A.
47. Aziz, S.G.-G.; Almasi, H. Physical Characteristics, Release Properties, and Antioxidant and Antimicrobial Activities of Whey Protein Isolate Films Incorporated with Thyme (Thymus Vulgaris L.) Extract-Loaded Nanoliposomes. *Food Bioprocess Technol.* **2018**, *11*, 1552–1565, https://doi.org/10.1007/s11947-018-2121-6%0A%0A.
48. Barbosa, L.N.; Rall, V.L.M.; Fernandes, A.A.H.; Ushimaru, P.I.; da Silva Probst, I.; Fernandes Jr, A. Essential Oils against Foodborne Pathogens and Spoilage Bacteria in Minced Meat. *Foodborne Pathog. Dis.* **2009**, *6*, 725–728, https://doi.org/10.1089/fpd.2009.0282.
49. Oliveira, T.L.C. de; Cardoso, M. das G.; Soares, R. de A.; Ramos, E.M.; Piccoli, R.H.; Tebaldi, V.M.R. Inhibitory Activity of Syzygium Aromaticum and Cymbopogon Citratus (DC.) Stapf. Essential Oils against Listeria Monocytogenes Inoculated in Bovine Ground Meat. *Brazilian J. Microbiol.* **2013**, *44*, 357–365, https://doi.org/10.1590/S1517-83822013005000040.
50. Cui, H.; Wu, J.; Li, C.; Lin, L. Promoting Anti-listeria Activity of Lemongrass Oil on Pork Loin by Cold Nitrogen Plasma Assist. *J. Food Saf.* **2017**, *37*, e12316, https://doi.org/10.1111/jfs.12316.
51. Hammer, K.A.; Carson, C.F.; Riley, T. V Antimicrobial Activity of Essential Oils and Other Plant Extracts. *J. Appl. Microbiol.* **1999**, *86*, 985–990, https://doi.org/10.1046/j.1365-2672.1999.00780.x.
52. Tayel, A.A.; El-Tras, W.F.; Moussa, S.H.; El-Sabbagh, S.M. Surface Decontamination and Quality Enhancement in Meat Steaks Using Plant Extracts as Natural Biopreservatives. *Foodborne Pathog. Dis.* **2012**, *9*, 755–761, https://doi.org/10.1089/fpd.2012.1203.
53. Burt, S. Essential Oils: Their Antibacterial Properties and Potential Applications in Foods—a Review. *Int. J. Food Microbiol.* **2004**, *94*, 223–253, https://doi.org/10.1016/j.ijfoodmicro.2004.03.022.
54. Shan, B.; Cai, Y.-Z.; Brooks, J.D.; Corke, H. The *in vitro* Antibacterial Activity of Dietary Spice and Medicinal Herb Extracts. *Int. J. Food Microbiol.* **2007**, *117*, 112–119, https://doi.org/10.1016/j.ijfoodmicro.2007.03.003.
55. Donsì, F.; Ferrari, G. Essential Oil Nanoemulsions as Antimicrobial Agents in Food. *J. Biotechnol.* **2016**, *233*, 106–120, https://doi.org/10.1016/j.jbiotec.2016.07.005.

56. Moghimi, R.; Ghaderi, L.; Rafati, H.; Aliahmadi, A.; McClements, D.J. Superior Antibacterial Activity of Nanoemulsion of Thymus Daenensis Essential Oil against E. Coli. *Food Chem.* **2016**, *194*, 410–415, https://doi.org/10.1016/j.foodchem.2015.07.139.
57. Jiménez, M.; Domínguez, J.A.; Pascual-Pineda, L.A.; Azuara, E.; Beristain, C.I. Elaboration and Characterization of O/W Cinnamon (Cinnamomum Zeylanicum) and Black Pepper (Piper Nigrum) Emulsions. *Food Hydrocoll.* **2018**, *77*, 902–910, https://doi.org/10.1016/j.foodhyd.2017.11.037.
58. Kim, I.; Lee, H.; Kim, J.E.; Song, K. Bin; Lee, Y.S.; Chung, D.S.; Min, S.C. Plum Coatings of Lemongrass Oil-incorporating Carnauba Wax-based Nanoemulsion. *J. Food Sci.* **2013**, *78*, E1551–E1559, https://doi.org/10.1111/1750-3841.12244.
59. Ahmad, M.; Benjakul, S.; Sumpavapol, P.; Nirmal, N.P. Quality Changes of Sea Bass Slices Wrapped with Gelatin Film Incorporated with Lemongrass Essential Oil. *Int. J. Food Microbiol.* **2012**, *155*, 171–178, https://doi.org/10.1016/j.ijfoodmicro.2012.01.027.
60. Kamona, Z.K.; Alzobaay, A.H.H. EFFECT OF ESSENTIAL OIL EXTRACT FROM LEMONGRASS (Cymbopogon Citratus) LEAVES ON VAIABILITY OF SOME PATHOGENIC BACTERIA AND SENSORY PROPERTIES OF FISH BALLS. *IRAQI J. Agric. Sci.* **2021**, *52*, 268–275, https://doi.org/10.36103/ijas.v52i2.1288.
61. Kieling, D.D.; Delarco, M.F.; Prudencio, S.H. Lemongrass Extract as a Natural Preservative of Cooked and Shredded Chicken Breast during Storage. *J. Culin. Sci. Technol.* **2021**, *19*, 55–66, https://doi.org/10.1080/15428052.2019.1703235.
62. Xu, Y.X.; Kim, K.M.; Hanna, M.A.; Nag, D. Chitosan–Starch Composite Film: Preparation and Characterization. *Ind. Crops Prod.* **2005**, *21*, 185–192, https://doi.org/10.1016/j.indcrop.2004.03.002.
63. Kieling, D.D.; Prudencio, S.H. Antioxidants Properties, Physicochemical, and Sensory Quality Attributes of a New Soy-Based Beverage with Lemongrass and Lime Juice. *J. Culin. Sci. Technol.* **2019**, *17*, 103–117, https://doi.org/10.1080/15428052.2017.1405859.
64. Olorunsanya, A.O.; Olorunsanya, E.O.; Bolu, S.A.O.; Adejumobi, C.T.; Kayode, R.M.O. Effect of Graded Levels of Lemongrass (Cymbopogon Citratus) on Oxidative Stability of Raw or Cooked Pork Patties. *Pakistan J. Nutr.* **2010**, *9*, 467–470, https://dx.doi.org/10.3923/pjn.2010.467.470.
65. Singh, A.; Mittal, A.; Benjakul, S. Chitosan, Chitooligosaccharides and Their Polyphenol Conjugates: Preparation, Bioactivities, Functionalities and Applications in Food Systems. *Food Rev. Int.* **2021**, 1–23, https://doi.org/10.1080/87559129.2021.1950176.
66. Tongnuanchan, P.; Benjakul, S.; Prodpran, T. Characteristics and Antioxidant Activity of Leaf Essential Oil–Incorporated Fish Gelatin Films as Affected by Surfactants. *Int. J. food Sci. Technol.* **2013**, *48*, 2143–2149, https://doi.org/10.1111/ijfs.12198.
67. Balakrishnan, B.; Paramasivam, S.; Arulkumar, A. Evaluation of the Lemongrass Plant (Cymbopogon Citratus) Extracted in Different Solvents for Antioxidant and Antibacterial Activity against Human Pathogens. *Asian Pacific J. Trop. Dis.* **2014**, *4*, S134–S139, https://doi.org/10.1016/S2222-1808(14)60428-X.
68. Lee, J.; Yang, H.; Lee, K.; Song, K. Bin Preparation and Application of a Flaxseed Meal Protein Film Containing Lemongrass (Cymbopogon Citratus) Oil. *Int. J. Food Sci. Technol.* **2016**, *51*, 1473–1480, https://doi.org/10.1111/ijfs.13121.
69. Wuryatmo, E.; Suri, A.; Naufalin, R. Antioxidant Activities of Lemongrass with Solvent Multi-Step Extraction Microwave-Assisted Extraction as Natural Food Preservative. *J. Funct. Food Nutraceutical* **2021**, *2*, 117–128, https://dx.doi.org/10.33555/jffn.v2i2.61.
70. Contini, L.R.F.; Zerlotini, T. de S.; Brazolin, I.F.; dos Santos, J.W.S.; Silva, M.F.; Lopes, P.S.; Sampaio, K.A.; de Carvalho, R.A.; Venturini, A.C.; Yoshida, C.M.P. Antioxidant Chitosan Film Containing Lemongrass Essential Oil as Active Packaging for Chicken Patties. *J. Food Process. Preserv.* **2022**, *46*, e16136, https://doi.org/10.1111/jfpp.16136.
71. Sacchetti, G.; Maietti, S.; Muzzoli, M.; Scaglianti, M.; Manfredini, S.; Radice, M.; Bruni, R. Comparative Evaluation of 11 Essential Oils of Different Origin as Functional Antioxidants, Antiradicals and Antimicrobials in Foods. *Food Chem.* **2005**, *91*, 621–632, https://doi.org/10.1016/j.foodchem.2004.06.031.
72. Naik, M.I.; Fomda, B.A.; Jaykumar, E.; Bhat, J.A. Antibacterial Activity of Lemongrass (Cymbopogon Citratus) Oil against Some Selected Pathogenic Bacterias. *Asian Pac. J. Trop. Med.* **2010**, *3*, 535–538, https://doi.org/10.1016/S1995-7645(10)60129-0.
73. Antunes, M.D.C.; Cavaco, A.M. The Use of Essential Oils for Postharvest Decay Control. A Review. *Flavour Fragr. J.* **2010**, *25*, 351–366, https://doi.org/10.1002/ffj.1986.

74. Sharma, A.; Sharma, N.K.; Srivastava, A.; Kataria, A.; Dubey, S.; Sharma, S.; Kundu, B. Clove and Lemongrass Oil Based Non-Ionic Nanoemulsion for Suppressing the Growth of Plant Pathogenic Fusarium Oxysporum f. Sp. Lycopersici. *Ind. Crops Prod.* **2018**, *123*, 353–362, https://doi.org/10.1016/j.indcrop.2018.06.077.
75. Chein, S.H.; Sadiq, M.B.; Anal, A.K. Antifungal Effects of Chitosan Films Incorporated with Essential Oils and Control of Fungal Contamination in Peanut Kernels. *J. Food Process. Preserv.* **2019**, *43*, e14235, https://doi.org/10.1111/jfpp.14235.
76. Wan, J.; Zhong, S.; Schwarz, P.; Chen, B.; Rao, J. Physical Properties, Antifungal and Mycotoxin Inhibitory Activities of Five Essential Oil Nanoemulsions: Impact of Oil Compositions and Processing Parameters. *Food Chem.* **2019**, *291*, 199–206, https://doi.org/10.1016/j.foodchem.2019.04.032.
77. Cofelice, M.; Cinelli, G.; Lopez, F.; Di Renzo, T.; Coppola, R.; Reale, A. Alginate-Assisted Lemongrass (Cymbopogon Nardus) Essential Oil Dispersions for Antifungal Activity. *Foods* **2021**, *10*, 1528, https://doi.org/10.3390/foods10071528.
78. Oh, Y.A.; Oh, Y.J.; Song, A.Y.; Won, J.S.; Song, K. Bin; Min, S.C. Comparison of Effectiveness of Edible Coatings Using Emulsions Containing Lemongrass Oil of Different Size Droplets on Grape Berry Safety and Preservation. *Lwt* **2017**, *75*, 742–750, https://doi.org/10.1016/j.lwt.2016.10.033.
79. Dewi, G.; Nair, D.V.T.; Peichel, C.; Johnson, T.J.; Noll, S.; Johny, A.K. Effect of Lemongrass Essential Oil against Multidrug-Resistant Salmonella Heidelberg and Its Attachment to Chicken Skin and Meat. *Poult. Sci.* **2021**, *100*, 101116, https://doi.org/10.1016/j.psj.2021.101116.
80. Ozge Can, F.; Durak, M.Z. Encapsulation of Lemongrass Oil for Antimicrobial and Biodegradable Food Packaging Applications. *Sci. Adv. Mater.* **2021**, *13*, 803–811, https://doi.org/10.1166/sam.2021.3941.
81. Kelen, M.; Tepe, B. Chemical Composition, Antioxidant and Antimicrobial Properties of the Essential Oils of Three Salvia Species from Turkish Flora. *Bioresour. Technol.* **2008**, *99*, 4096–4104, https://doi.org/10.1016/j.biortech.2007.09.002.
82. de Oliveira, M.M.M.; Brugnera, D.F.; das Graças Cardoso, M.; Alves, E.; Piccoli, R.H. Disinfectant Action of Cymbopogon Sp. Essential Oils in Different Phases of Biofilm Formation by Listeria Monocytogenes on Stainless Steel Surface. *Food Control* **2010**, *21*, 549–553, https://doi.org/10.1016/j.foodcont.2009.08.003.
83. Ahmad, M.; Benjakul, S.; Prodpran, T.; Agustini, T.W. Physico-Mechanical and Antimicrobial Properties of Gelatin Film from the Skin of Unicorn Leatherjacket Incorporated with Essential Oils. *Food Hydrocoll.* **2012**, *28*, 189–199, https://doi.org/10.1016/j.foodhyd.2011.12.003.
84. Yang, H.-J.; Song, K. Bin Application of Lemongrass Oil-Containing Polylactic Acid Films to the Packaging of Pork Sausages. *Korean J. Food Sci. Anim. Resour.* **2016**, *36*, 421, https://doi.org/10.5851%2Fkosfa.2016.36.3.421.
85. Han Lyn, F.; Nur Hanani, Z.A. Effect of Lemongrass (Cymbopogon Citratus) Essential Oil on the Properties of Chitosan Films for Active Packaging. *J. Packag. Technol. Res.* **2020**, *4*, 33–44, https://doi.org/10.1007/s41783-019-00081-w.